Université de Montréal

The Effects of Crystallization on the Pulsations of White Dwarf Stars

by

Dominique Paradis

Département de physique

Faculté des arts et des sciences

Thesis presented to la Faculté des études supérieures

so as to obtain the title of

Master of Sciences (M.Sc.)

in physics

May, 2004

Université de Montréal

Faculté des études supérieures

This thesis entitled:

The Effects of Crystallization on the Pulsations of White Dwarf Stars

presented by:

Dominique Paradis

was evaluated by a jury composed of the following people:

Pierre Bergeron, président-rapporteur

Gilles Fontaine, directeur de recherche

Pierre Brassard, membre du jury

Thesis accepted on the: _____

Abstract

The theory of white dwarf crystallization has been around for over forty years, yet there exists few direct observational tests to verify it. A little over a decade has past since a possible testing-ground for the theory has been discovered, the star BPM 37093, yet our ability to proceed with such tests using current methods is still under debate. This DAV star has the characteristic pulsations of the others of its type, yet it also has a mass high enough so that, by theoretical calculations, we expect the center to already be in the process of crystallizing, leading some to propose that the pulsations could serve as indicators of the crystallized fraction of the star. The valididity of this claim, the use of current techniques and stellar knowledge, to determine the exact fraction of the star which is crystallized is the basis of this research. Using extensive, and careful modeling techniques, the relative importance of the crystallization as a parameter of pulsation is determined and compared versus the other stellar parameters. This allows for a quantitative analysis of the use of the observed variations in the determination of the nature of the crystallized core. The final result of this research is that our inability to correctly determine another important parameter of pulsation negates any possibility of capitalization of the effects created by the crystallization, and therefore makes it impossible to accurately probe the interior of BPM 37093.

Keywords: BPM 37093, crystallization, white dwarf oscillations

Sommaire

Bien que la théorie de la cristallisation des naines blanches existe depuis plus de quarante ans, elle ne fut vérifiée directement par l'observation qu'à peu de reprises. BPM 37093, une étoile naine blanche DA variable découverte il y plus de dix ans pourrait être la solution à ce problème, mais un débat existe toujours à savoir s'il serait possible de prouver la théorie avec les méthodes actuelles. Dû à sa masse élevée, les modèles d'évolution démontrent que le centre de BPM 37093 doit être cristallisé. De plus, le fait que BPM 37093 soit une étoile variable permet de la soumettre à une analyse plus poussée, sondant le centre de l'étoile et étudiant directement la cristallisation. Cette procédure nous laisserait donc une connaissance améliorée d'une étape majeure dans la vie des étoiles naines blanches. Il a été proposé que l'étude des variations d'intensité lumineuse, par l'application de nos connaissances actuelles, puisse nous permettre de découvrir la nature exacte de la partie cristallisée. Cette recherche se veut une réponse à cette suggestion. En utilisant des techniques de modélisation établies, l'importance relative de la cristallisation comme paramètre de pulsation va être déterminée et comparée à celle des autres paramètres stellaires. Ceci nous permettra donc déterminer si l'observation des pulsation est suffisante pour bien caractériser la nature du centre cristallisé. Malheureusement, nous concluons par la négative, la marge d'erreur sur un autre des paramètre de pulsation étant suffisament grande pour affecter le comportement des modèles. La possibilité de sonder directement l'intérieur de BPM 37093 correctement n'est toujours pas à notre portée.

Mots clé: Astrophysique, Étoiles individuelles;BPM 37093, Cristallisation, Oscillations, Naines blanches

Table of contents

List of figures

List of tables

Chapter 1

Introduction

When a star exhausts the fuel required for thermonuclear reactions, the pressure created by the heat of the reactions to oppose gravitational contraction ceases and the stellar core begins to collapse. For an average star, specifically those with a mass equivalent or smaller than about eight times that of the Sun ($8M_{\odot}$), during this process of gravitational collapse the outer layers, which consist of a large portion of its mass, are thrown off forming a planetary nebula. As the plasma of the collapsing core continues to increase in density, the available energy levels of the free electrons start to fill up. Due to the Pauli Exclusion Principle, which states that no two identical electrons can occupy the same energy level, a force known as the degenerate electron pressure is created so as to oppose further contraction of the gas, thus stopping electrons from being crowded together in a manner so as to violate this quantum mechanical principle. After the star has succumbed to a critical amount of collapse this opposing force becomes strong enough to stop gravitational contraction completely, and the hot stellar core becomes a degenerate star known as a young white dwarf featuring a surface temperature well in excess of $100,000K$.

An average white dwarf has a mass of $\sim 0.6M_{\odot}$ and a radius slightly larger than that of the Earth. This indicates an enormous average density on the order of 10^6 g/cm^3 (note the average density of the Earth and Sun are only 5.5 g/cm^3 and 1.4 g/cm^3 respectively). Other than allowing for such an enormous gas density, the nature of the white dwarf as degenerate star creates a unique correlation between its mass and radius. As the mass of the

star is increased, the gravitational force becomes much stronger, overpowering the electron degeneracy pressure and contracting the gas. The electrons contained within are forced closer together, and through the Pauli Exclusion Principle subsequently increase the strength of the electron degeneracy pressure until equilibrium is achieved. The increase of the mass of the star requires a greater opposing force to be created, due to the nature as a degenerate star, this can only be provided by a decreasing the space between electrons in the method described above, therefore as a white dwarf increases in mass its size must decrease, contrary to stars supported by thermonuclear reactions. The intense gravitational field present in these stars also forces them to be extremely chemically stratified, with the heavier elements being much more affected, sinking quicker towards the center.

Since there are no thermonuclear reactions left within white dwarfs, there is therefore no way for them to replenish their internal heat (unless they accrete further matter from a nearby star) and the whole of their evolution consists of a cooling process. Due to their small surface from which their stored energy can be radiated though, the initial heat present at their formation lasts for billions of years. Eventually, after all of the latent energy is radiated out of the white dwarf, it will cool to form a cold solid body known as a black dwarf. Though the idea of a black dwarf is theoretically sound there are none in existence at this time so as to verify it. This is known based on our estimate on the age of the universe versus our estimates on the time required for a star to: form due to gravitational collapse of ambient material, burn all of its nuclear fuel, become a white dwarf, and then radiate all of its stored energy to the surrounding space. The universe has not existed long enough for this full process to have occurred in any star with an initial mass $M_i < 8M_\odot$, the limit for white dwarf formation.

Though the electron degeneracy pressure formed by the white dwarfs to oppose gravitational collapse is strong, there is a limit to the mass of the object which can be supported by this process, and it is known as the Chandrasekhar limit. If the mass increases above this critical mass ($\sim 1.4M_\odot$), usually through the process of accretion of material from a neighbouring star, the internal pressure is no longer strong enough to oppose the gravitational collapse, causing the whole star to explode as a type I supernova, the most massive type of supernova known. Though the Chandrasekhar limit is universal, it does not hinder stars with initial

masses greater then $1.4M_{\odot}$ to become white dwarfs since most of their stellar mass is lost in stellar wind episodes of the red giant phase and, finally, in the planetary nebula phase.

In essence a white dwarf is a non-main sequence star which is supported against gravitational collapse by an electron degeneracy pressure. Over the years since the first one was discovered, many white dwarfs have been observed and catalogued into a large variety of groups, all with different physical properties. Even with these well established groups, there are still a few stars which are unique, with characteristics or combinations of them unseen in any other. One of these is BPM 37093, the topic of this research. As a member of the DAVs (discussed in detail in Section 2.2), a known group of pulsating white dwarfs, this star initially appeared as any other of this group, yet one of its physical characteristics sets it apart from the rest, its high mass. This physical parameter is so large that, even at its high temperature (for the process) it has a crystallized core (discussed in detail in section 3.6), while still exhibiting the variations characteristic of its stellar category. This makes BPM 37093 the only known star in this important step in white dwarf evolution which is also pulsating, a characteristic which normally allows the interior of stars with it to be probed using asteroseismology. It has been proposed that using current techniques, it would be possible to use the observed variations in the BPM 37093's light curve to determine the exact nature (i.e. mass and composition) of its crystallized component. The purpose of this research is to determine the validity of this claim. Through use of extensive stellar modelling, the relative effects of varying the fraction of crystallization of the star will be compared to those caused by the variation of the other stellar parameters, such as the effective temperature, surface gravity, thickness of the helium layer, thickness of the hydrogen layer, convective efficiency, as well as core composition. Due to specific, and known, uncertainties on the physical parameters of the star, the above comparison can be used to determine if current methods are indeed sufficient enough for an accurate determination of BPM 37093's nature.

Chapter 2

Pulsating DA White Dwarf Stars (DAV's)

In stellar research it is important to understand the category within which the particular star in question is found, for BPM 37093 this is the DAV or ZZ Ceti category. To fully understand these intricate objects a broader vision is required, leading to the initial discussion based of the DA stellar class for which the DAVs are a subgroup.

2.1 DA stars

A DA star is a white dwarf whose spectrum is dominated by strong hydrogen lines. In the stellar evolutionary process involved in the formation of a white dwarf, approximately three-quarters of the stars retain a thin shell of hydrogen on the surface, thus creating white dwarf stars with spectra almost devoid of all other elements. These hydrogen-line stars are found in a very large temperature range from $100,000K$ to $5,000K$, thus allowing the observed hydrogen lines to be in a large variety of forms from fairly shallow (for the hottest stars) to very sharp (for the coldest stars).

As previously mentioned in chapter 1 for all white dwarfs, there is an extreme chemical stratification present in these stars, for DAs specifically this leads to a rather simple physical structure consisting of a massive core composed of a mixture of carbon and oxygen which

contains approximately 99% of the mass of the star, a thin layer of helium about 100 km thick surrounding the core, and finally an outer hydrogen layer approximately 1 km thick enveloping everything else. The outermost region of this last thin layer, whose purity is maintained by the intense gravitationally-induced chemical stratification, is the location of Balmer transitions in hydrogen, or excitations originating from the first excited level ($n = 2$) of the atom. This process is practically the only source responsible for the formation of the stellar spectra, thus creating the characteristic hydrogen dominated signature of this category of stars.

2.2 DAV or ZZ Ceti stars.

Within the very large group of degenerate stars known as the DAs, are found the DAV or ZZ Ceti stars. Having the same physical characteristics as other DAs, only one observable anomaly makes them stand apart, the fact that their luminosities vary with time. The name itself, DAV quite simply stands for the fact that they are DA stars with observed variations (thus the V is added for this distinction). The first of these intriguing objects to be discovered, HL Tau 76, was done so accidentally by Landolt (1968). Previously only considered as a blue variable star, it was later discovered that it could also be classified as a DA white dwarf star. From this discovery a new stellar class was formed and dubbed the DAVs, or ZZ Ceti stars after the renamed prototype.

As variable stars which form a subgroup, and possibly an evolutionary phase, of the most numerous type of degenerate stars, the DAVs can serve as important observation points to the internal structure of white dwarfs. By studying their pulsations the insides of these stars can be sounded, much like the internal structure of the Earth can be mapped using seismological methods. This Earth based technique, which analyzes the interaction of pulsations passing through our planet with Earth's internal structure, lends its name to its stellar counterpart, giving us asteroseismology as a tool to probe the interior structures of pulsating stars. Much as the name implies this method uses the pulsations of the white dwarf and their interactions with the structure of the star to probe its chemical stratification and layout. By determination of the rates at which the periods of these pulsations change, a process which is very sensitive to the chemical composition of the environment within which they are propagating, global

chemical structures of the star can be determined, such as the core composition of the white dwarf. Also due to the susceptibility of the period distribution to the chemical stratification of the system, by careful observation it is possible to acquire an accurate determination of the mass of the external envelopes of hydrogen and helium.

2.2.1 Pulsations

Physically, these stars are perfectly ordinary DA white dwarfs save for their variability caused by non-radial g-mode instabilities, that is instabilities where gravity is the restoring force. The physical manifestation of these pulsations, which are created by the superposition of pulsation modes, is temperature waves, like deformations, which move across the surface of the star in primarily horizontal motions. The effect of this phenomenon is multi-periodic luminosity variations in the light curves on the order of 0.003 to 0.300 magnitude, with observed periods within the range of 100-1200 seconds.

The formation of these pulsations is directly dependant on the physical characteristics of these stars. Within the temperature range where the ZZ Cetis are found, a narrow domain approximately centered around $11,500K$, hydrogen, the sole component of the outer layer of the star, begins to recombine, leading to the formation of a partial-ionization induced convective zone and thus an increase in the opacity of this thin layer. All of these factors together drive the creation of g-modes, which when superimposed upon one another form the observed luminosity variations of these stars. As the DAV star cools this partial-ionization zone of hydrogen moves deeper into the star extending the thermal timescale and thus increasing the energy which is available to drive further pulsations. As discussed in Kanaan et al. (1998) this situation leads to a correlation between the temperature, the amplitude of the pulsations and the observed periods, implying that the cooler a star is the larger the amplitudes and periods of its pulsations will be. Of particular interest for this discussion is the situation at the red or cool edge of the instability strip (described in section 2.2.2) where BPM 37093 is found, these stars generally have many long period modes (600s or more) and large amplitudes, but what is of more interest is the fact that they demonstrate intrinsic instabilities, causing the pulsation modes to change over periods of months or weeks.

2.2.2 The Instability Strip

From an early study based upon 7 known ZZ Cetis by McGraw & Robinson (1976), all of the DAVs seem to form a highly homogeneous group in the $\log g - T_{eff}$ plane centered around $T_{eff} = 11,500K$, consistent with the idea that the pulsations are driven by the recombination of hydrogen. Further research, specifically by Fontaine et al. (1982) using multi-channel photometric data, concluded that the DAVs could reside in a pure instability strip void of non-variable white dwarfs, implying that the DAV phase is an evolutionary step through which all DA stars must pass as they cool. As of Bergeron et al. (2004) there are 36 known ZZ Ceti stars, and interestingly enough in accord with the conclusion presented above, they are all found within a very small temperature range from $11,100K \leq T_{eff} \leq 12,500K$ where no other types of stars are found. Therefore the idea of a pure instability strip seems to hold its ground.

Figure 2.1, taken with permission from Fontaine et al. (2003b), demonstrates the location of the instability strip within the $\log g - T_{eff}$ plane. The open circles represent constant, non-variable stars, while the filled circles in the figure represent 28 of the 32 then known ZZ Ceti stars, while not using the 4 others due to the poor optical spectra used in their parameter determination. Also of particular interest in this figure is the solid and dashed lines which represent the empirical and theoretical boundaries of the ZZ Ceti instability strip, where the later was created with the inclusion of the appropriate convection model. The dotted curves which are seen horizontally across the figure represent the evolutionary tracks of hydrogen atmosphere white dwarfs of specific masses. Lastly the open circle found on the edge of the instability strip indicated with "bin?" is an unresolved degenerate binary and as such can be ignored.

As seen in figure 2.1, the instability strip seems to be a trapezoid shaped region in the $\log g - T_{eff}$ plane, with the blue edge demonstrating a strong dependence on the surface gravity of the stars. Within the appropriate margins of error it can accurately be said that there are no non-variable stars within the ZZ Ceti instability strip, this is also seen in the research by Bergeron et al. (2004) in which the latest known DAVs are also considered. All of this confirms the idea that the instability strip is in fact a pure one, and that the DAVs

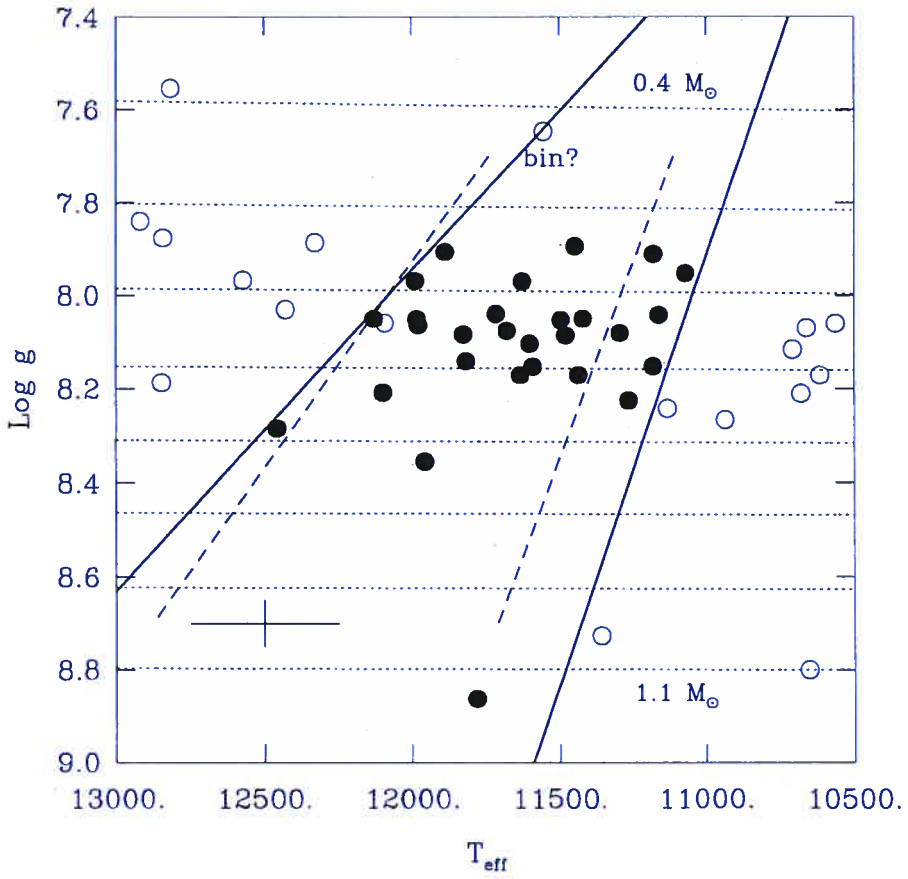

FIGURE 2.1 – DAV instability strip in T_{eff} vs. $\log g$ plane taken with permission from Fontaine et al. (2003b)

themselves are an evolutionary phase through which all DA white dwarfs must pass, remaining consistent with the conclusion proposed over 20 years ago by Fontaine et al. (1982).

2.2.3 Optical Spectroscopic approach

In the case of BPM 37093, as with a large number of DAVs, the method which was used for the acquisition of its most accurate estimates of its physical properties, the effective temperature and the mass, is the optical spectroscopic approach. This method uses the direct comparison of the Balmer lines, from Hβ to H9, of high signal-to-noise spectroscopic observations, to those predicted using highly accurate stellar models, whose physical parameters are

known.

The first instance of use of this method was by Bergeron & McGraw (1990) for the star GD 165, but the theoretical framework for measuring the T_{eff} and the $\log g$ of DAVs was developed by Bergeron et al. (1995), considered to be the most comprehensive and homogeneous study of the ZZ Cetis published to date. The continued research from this article has great importance since it provides a homogeneous group within which direct comparisons are appropriate due to the use of similar (yet ever improving) model atmospheres at every step.

There have been some critics of this method, most notably Koester & Allard (2000), claiming that the accuracy of the process creates a margin of error for the effective temperature on the order of $2000K$, much larger than the width of the instability strip thus making the research inconclusive. Fontaine et al. (2003a), though irrevocably refutes all of the accusations against this method, as well as proving that the optical spectroscopic approach alone could lead to accurate estimates of the effective temperature and mass of these stars. In all, as of this article, with consistent data and homogeneous methods the optical spectroscopic approach had uncovered seven ZZ Cetis with 100 percent predictive power, a record unmatched for the DAVs.

2.2.4 The Brunt-Väisälä Frequency

The configuration of the g-modes within pulsating stars is determined by a crucial parameter known as the Brunt-Väisälä frequency, which takes the form (equation 14 from Brassard et al. (1991)):

$$N^2 = \frac{g^2\rho}{P}\frac{\chi_T}{\chi_\rho}\left(\nabla_{ad} - \nabla + B\right) \tag{2.1}$$

This therefore indicates that the frequency (N) is a function of certain physical properties of the environment, including; the pressure (P), the density (ρ), and the actual and adiabatic temperature gradients (∇ and ∇_{ad} respectively). Stellar models indicate that these factors are directly dependent on the effective temperature (T_{eff}), the surface gravity (g which is also present in equation 2.1) and the chemical composition of the star. Apart from these stellar physical parameters N is also dependent on another factor of particular interest, B, which

has the form:

$$B \equiv -\frac{\chi_Y}{\chi_T}\frac{d}{d}\frac{\ln Y}{\ln P} \tag{2.2}$$

Where the compressibility parameters (χ_Y, χ_T, and χ_ρ) of a material with a specified chemical composition can be expressed as:

$$\chi_Y = \left(\frac{\delta \ln P}{\delta \ln Y}\right)_{\rho,T} \tag{2.3}$$

$$\chi_T = \left(\frac{\delta \ln P}{\delta \ln T}\right)_{\rho} \tag{2.4}$$

$$\chi_\rho = \left(\frac{\delta \ln P}{\delta \ln \rho}\right)_{T} \tag{2.5}$$

For DAVs, there are two transition zones between areas of different chemical compositions; the area of interaction between the outer hydrogen layer with the helium layer, and that of the helium layer with the stellar core. For the above formulation of the B factor, Y represents the mass fraction of helium, and due to its involvement in both of the transition zones it can be used as an indicator of chemical change, thus making χ_Y the only compressibility parameter solely based on the changing of chemical composition, while χ_T (and χ_ρ in equation 2.1), also a function of the composition, represents the compressibility due to the temperature (density). From B's direct dependence on two different chemically specific parameters (χ_Y and χ_T), it is evident that this parameter only becomes pertinent at transition zones between two areas of different chemical compositions.

Overall the Brunt-Väisälä frequency is the determinant of the configuration of the pulsation modes found within pulsating DA stars, and contained within its determination are all of the physical components of the star, be it either the direct dependence on the pressure or temperature gradients (found in equation 2.1), or the more subtly present chemical composition of the layers (as expressed by the B factor).From the determination of this parameter, the dependance of its pulsations to the physical parameters of a star can be exposed, therefore

the Brunt-Väisälä frequency plays a key role in asteroseismology.

2.2.5 Effects of Stellar Parameters to the Pulsations

Using the theory presented in section 2.2.4, predictions on the effects to the pulsations of varying the stellar parameters can be made, and was done in great detail in the comprehensive work of Brassard et al. (1992a). Using the same numerical designations for the predictions as those assigned in the above article, table 2.1 presents the expected results of varying four specific stellar parameters, the thickness of the hydrogen layer, the convective efficiency, the stellar mass, and the effective temperature.

effect	prediction	parameter change
average period spacing between adjacent modes increases with:	2	decreasing Hydrogen layer mass
	3	increasing convective efficiency
	4	decreasing Mass
	5	decreasing effective temperature T_{eff}
average period spacing between consecutive trapped modes increases with:	6	decreasing Hydrogen layer mass
	7	increasing convective efficiency
	8	decreasing Mass
	9	decreasing effective temperature T_{eff}
period of a given pulsation mode increases with:	10	decreasing Hydrogen layer mass
	11	increasing convective efficiency
	12	decreasing Mass
	13	decreasing effective temperature T_{eff}

TABLE 2.1 – predictions of pulsating properties of DA white dwarf stars, from Brassard et al. (1992a)

Chapter 3

BPM 37093

BPM 37093, also known as LTT 4816, can be found in the constellation Centaurus at a distance or approximately 54 light-years (or 17 parsecs), and is unique within the vast catalogue of stars which have been recorded. When initially observed to pulsate, by Kanaan et al. (1992), it resembled an ordinary ZZ Ceti star, further analysis of its physical properties though, specifically by Bergeron et al. (1995), indicated that its mass was extremely elevated. Theoretical models involving the known mass and effective temperature indicated that BPM 37093 was partially crystallized, making it the only white dwarf in this phase of cooling which exhibits pulsations, and therefore the only known possible candidate where the theory of crystallization could be directly tested. It has been proposed that asteroseismological probing of its interior could allow for a direct determination of BPM 37093's crystallized mass, and therefore a better comprehension of this important phase of the cooling process. This improved understanding of the crystallization process would allow for more accurate age determinations of older white dwarfs, who are important cosmochronological tools, therefore making it possible that BPM 37093 could potentially have a direct influence on the generally accepted age of the universe. Though the possibilities of this probing is the main topic of this research, the direct purpose of this chapter is a general overview of BPM 37093 itself, including the values of the physical parameters which will be used in the stellar models presented in subsequent sections.

3.1 Effective Temperature T_{eff}

As discussed in section 2.2.3, the optical spectroscopic approach is used in the determination of the physical properties of ZZ Ceti stars by fitting the Balmer lines of observations to those of stellar models. In this capacity figure 3.1 is a Bergeron diagram of BPM 37093 for the Balmer lines from $H\beta$ to $H9$, graciously provided by Pierre Bergeron for use in this research.

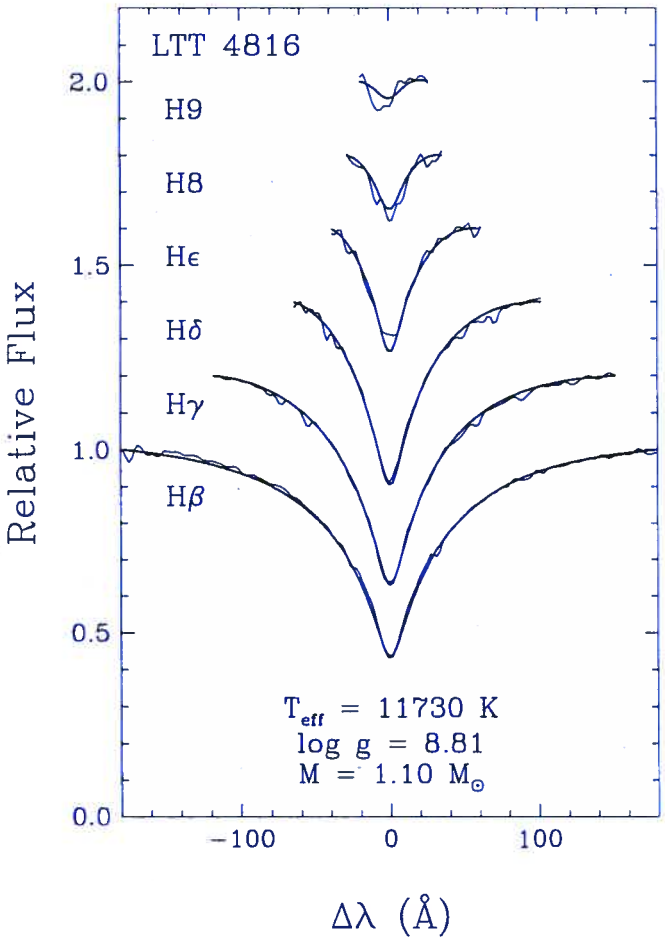

FIGURE 3.1 – Bergeron diagram of BPM 37093, for fits with the Balmer lines from $H\beta$ to $H9$

Initial analysis of BPM 37093 with this method by Bergeron et al. (1995) gave a result for the effective temperature of $T_{eff} = 11,730K$, as in figure 3.1, with a margin of error of $\pm 350K$. Since that time, further study by Fontaine et al. (2003a) of the optical spectroscopic

approach has been able to determine that the margin of error for this method in much smaller than that initially indicated in the aforementioned article, leading to the value used from now on in this research:

$$T_{eff} = 11730 \pm 200K$$

3.2 Surface Gravity $\log g$

From the same analysis used to determine the effective temperature, represented in figure 3.1, the value of the surface gravity ($\log g$) of BPM 37093 can be determined. As initially stated in Bergeron et al. (1995), with the margin of error confirmed by Fontaine et al. (2003a), the value for BPM 37093 is:

$$\log g = 8.81 \pm 0.05$$

Stellar evolution models with thick hydrogen layers associate this surface gravity with a stellar mass of:

$$M = 1.10 \pm 0.065 M_{\odot}$$

which itself is confirmed by research done by Giovannini (1996), using completely different model atmospheres.

From figure 2.1 using the effective temperature and surface gravity discussed here, it is clear that BPM 37093 is found well outside the tight group consisting of all the other DAVs located at much lower masses. The next most massive DAV, as of Bergeron et al. (2004), is 0632-5605 with a mass of $M = 0.92 M_{\odot}$, significantly lower than that determined for BPM 37093.

3.3 Thickness of the Hydrogen Layer $\log q(H)$

The thickness of the hydrogen layer ($\log q(H)$) is a term used to refer to the mass of the outer hydrogen layer surrounding the star, mathematically represented in equation 3.1, where $M(H)$ and M_* are the total mass of hydrogen present in the layer and the total stellar mass

respectively.

$$\log q(H) = \log [M(H)/M_*] \tag{3.1}$$

Unlike the two previous physical parameters it is not possible to directly observe the thickness of the hydrogen layer, thus requiring purely theoretical limits to the parameter. Stellar evolutionary theory predicts that the maximum amount of hydrogen which can survive the nuclear burning of the planetary nebula phase of white dwarfs evolution is only 10^{-4} of the stars complete mass, giving the range to be used for the thickness of the hydrogen layer as:

$$-9 \leq \log q(H) \leq -4$$

Since the believed value of $\log q(H)$ should fall around -4.5 to -5, the lower limit to this parameter space is set at such a low value (-9) so as to have a complete view of the situation at hand, while remaining high enough so that there are no numerical problems due to the requirement of hydrogen in the atmosphere for the desired chemical stratification in the stellar models.

3.4 Thickness of the Helium Layer $\log q(He)$

Much like the hydrogen layer, the thickness of the helium layer $(\log q(He))$ can be represented as:

$$\log q(He) = \log [M(He)/M_*] \tag{3.2}$$

with $M(He)$ representing the mass of the helium in the inner layer around the stellar core. As with the hydrogen layer the boundaries imposed upon this parameter must be based upon theoretical research, where the maximum limit is dictated by the amount of the helium which can survive nuclear burning in the planetary nebula, and a lower one dictated by the chemical stratification and its effect to the coupling of the hydrogen and helium layers. This leaves the parameter space to be used in this research as:

$$-4 \leq \log q(He) \leq -2$$

3.5 Observations of BPM 37093

Observationally, BPM 37093 is a DA6 spectral class star with an absolute visual magnitude of magnitude $M_V = 12.87$, total luminosity of $L = 6\text{x}10^{-4}L_{\odot}$, and as per Kanaan et al. (1998) has a light curve dominated by low amplitude pulsations of only 5 mmag. Also, like the other DAVs found on the red-edge of the instability strip, there are noticeable instabilities in its pulsation modes, uncharacteristically for this type of DAV though, the variations occur over a period of days, not the usual weeks or months. Throughout the literature there is no clear explanation as to why this is so, but it is possible that the nature of BPM 37093 as a crystallized pulsator could be the cause.

Year Detected	Period (s)	Year Detected	Period (s)
1991	609	1998	601
1991	546	1998	582
		1998	565
1992	608	1998	563
		1998	548
1995	617		
1995	565	1999	633
		1999	549
1996	649	1999	531
1996	582	1999	512
1996	566		
1996	532	2003	635.1
		2003	613.5
1997	604	2003	600.7
1997	560	2003	582.0
		2003	564.1
1998	637	2003	548.4
1998	633	2003	531.1
1998	614	2003	511.7

TABLE 3.1 – the observed periods of BPM 37093, taken from Kanaan et al. (2000) with added data from Metcalfe et al. (2004)

Table 3.1, which presents the observed pulsations of BPM 37093 and the year within which they were recorded, demonstrates that in accordance with the other red-edge DAV stars,

BPM 37093 has pulsations with long periods, averaging around 600 seconds. As mentioned in section 2.2.1 though, the pulsations of these stars on the cool boundary of the instability strip should also have large amplitudes, which is not the case from BPM 37093 . With the theoretically predicted correlation in other DAVs between the effective temperature and the amplitude and periods of the pulsations, BPM 37093 should have stopped pulsating earlier, since this is obviously not the case, furthur analysis of the situation is required.

Also of particular interest is the intrinsic instability present in BPM 37093, in that its pulsation modes disappear and return periodically over a period of days. Though all of the other red-edge ZZ Cetis follow similar patterns, usually this occurs over periods of weeks or months, never over in a time span as short as that of BPM 37093. It has been proposed in Kanaan et al. (1998) that this rapid variability could be an indication that the pulsations within the star are being shut-down and it is on its way out of the instability strip as a non-variable star, but this theory cannot be tested as of yet. Also a particularity arises in the analysis of the total power output of BPM 37093 versus other DAVs, as seen in Kanaan et al. (1998), in that it is much lower then that produced by other DAVs of the same temperature.

Purely based on the photometric analysis presented above the differences between BPM 37093 and the other ZZ Ceti stars are quite evident and fundamental. Though there are no definitive explanations for these differences, it could be possible that they are solely based on the fact that it is a crystallized while the others are not. If in fact this is true, these characteristics could be used as sign posts for the determination of the presence of crystallization in other pulsating DAVs. The current applicability of this knowledge remains rather small though since BPM 37093 is the only known candidate of this type. Alternatively, the unusual pulsation properties of the star may be solely due to its high surface gravity, without the implication of the crystallization.

3.6 Crystallization

For over forty years, since the research by Salpeter (1961), it has been widely accepted that all white dwarfs must eventually crystallize, a process in which their liquid compositions become solid. As a white dwarf cools past a certain critical temperature, determined by its

mass, the thermal energy of its layers (starting from the core and proceeding outwards as time progresses) becomes insufficient to counteract the electrostatic interactions between the individual ions. As these interactions take control, the ions reconfigure themselves and bind with their neighbours, locking the whole system as a solid structure. The final product, after the whole star has undergone this process, is a solid sphere known as a black dwarf.

Theoretical models involving BPM 37093's effective temperature and surface gravity have predicted that it has already begun the process of crystallization, with the predicted crystallized mass fraction (M_{xtal}/M_*) of the star varying depending on the chemical composition of the core used in the models. In the article by Winget et al. (1997) the results of some of these theoretical models are presented, giving a value to M_{xtal}/M_* of 0.50 for a pure carbon core, 0.90 for a pure oxygen core and even greater value if the core is composed of heavier elements such as neon. Being that BPM 37093 is the first of its kind as a possible testing ground for the theory of crystallization, there are no other cases with which to refer it, therefore a general discussion of the predictions on the implications of the crystallization to the pulsations is called for.

The first study using asteroseismology to determine if crystallization would have an effect on the pulsations was done by Hansen & van Horn (1979), well before BPM 37093 was even discovered. The primary concern of this article was within the range of normal mode periods, and did not include high overtone g-modes as observed in BPM 37093, therefore the results of the study are not applicable to the subject at hand. Another study by Montgomery & Winget (1998) though, predicts that due to the global nature of the g-modes, the presence of a solid boundary in the core would affect the pulsations enough that they would be observably different then those in a star that is not crystallized whatsoever. The determination of the validity of this last proposition is the purpose of this research and will be discussed in the next chapter.

Chapter 4

Calculations and Results.

To be able to have a better understanding of the physical processes at work within BPM 37093 an in-depth study of this star must be conducted. By creating static numerical models, and then applying a pulsation code to them it is possible to determine the effects that each of the parameters of the star has to the pulsations created. So as to achieve this end many models of the star were created, each with a slight variation to one of the parameters of pulsation; the effective temperature (T_{eff}), the surface gravity ($\log g$), the thickness of the Hydrogen layer ($\log q(H)$), the thickness of the Helium layer ($\log q(He)$), the convection theory used, the chemical composition of the core, and the fraction of the star that is crystallized. By analyzing the effects to the pulsation that is caused by varying these parameters within the appropriate limits the overall importance of each of these parameters can be compared. From this analysis it will be possible to determine which uncertainty on the value of the parameters causes the most variation to the pulsations, and therefore determine the effectiveness of using the stellar pulsation models as a tool for direct determination of these physical parameters of the star.

Due to the fact that BPM 37093 is the only known crystallized white dwarf for which variations have been observed, it can be proposed that an asteroseismological study of the pulsations could be used so as to probe the interior of the star and determine the fraction that is crystallized. With the method of modellization described above, and shown in detail in this chapter, the importance of the fraction of crystallization to the observed pulsations

can be determined. If in the end it is discovered that this is the major contributor to the pulsations, then the above method could be worked out in reverse from the observations and a direct constraint to the fraction of crystallization could be made. With this an even better understanding of the crystallization of white dwarfs could be achieved therefore better explaining one of the major events in the cooling of these degenerate stars.

4.1 Stellar Model and Pulsation Codes used.

So as to create the stellar models used throughout this research an upgraded version of the model-building code described by Brassard & Fontaine (1994) was used. All of the configurations for this code for DAV white dwarfs remained constant throughout the research thus creating an environment where direct comparisons are possible.

The latest version of the pulsation code presented in Brassard et al. (1992b) was used on these static models so as to create realistic pulsations within the created system. This code, applicable for adiabatic situations, uses the Galerkin finite-element method (GFEM) so as to solve the boundary-value problems for ordinary differential equations present in non-radial stellar pulsations. For complete details on the code and the solution methods used by it for the equations of pulsation, please refer to the previously mentioned reference.

4.2 Determination of the Wave number (l).

Stellar pulsations can closely be represented using spherical harmonics. The complexity of the situation is greatly reduced due to the great distance at which the star is observed, allowing for only the variations over the surface area perpendicular to the observer to be analysed. This simplification, combined with the fact that we cannot resolve this visible disk due to the distance, allows for a geometric cancellation effect to occur, reducing of the amount of spherical harmonic indices required to describe the system to only one, the latitudinal wave number (l), and limiting this index to small values. Determination of this wave number is important so as to be able to properly analyse the pulsations of BPM 37093, and has been attempted in a few different studies.

The first attempt to identify the wave number of the pulsations of BPM 37093 is presented in Dreizler et al. (2000). Since there is only a small amount of known pulsations for the star they state that the usual method of comparison of theoretical models to observations so as to determine the wave number cannot be used. The method that they do attempt to use involves the limb-darkening method (described in the article) so as to determine the brightness distribution of the star and therefore the wave number. The full details of this method are not covered here since the final conclusion in this paper is that the signal to noise (S/N) ratios of the observations are too low, therefore disallowing the application of the method to determine l.

The next attempt at determining the wave number of the pulsations can be seen in Nitta et al. (2000), where they also use the limb darkening method but this time combined with the data obtained from the Whole Earth Telescope (WET) (in April 1999) and the Hubble Space Telescope (HST). The preliminary results from analysis of the four observed modes at the time was that the wave number of the pulsations are not $l \geqslant 3$. The exact value of the wave number (either $l = 1$ or $l = 2$) could not be determined from the data though since their is one important problem with this technique, it assumes that the modes in the star can be described perfectly by spherical harmonics. Since we cannot be absolutely sure that this is the case (but we think it is rather close) we must look elsewhere for further restrictions of the wave number.

Lastly in Kanaan et al. (2000) they combine the observed periods, seen in table 3.1 into nine periods (combining periods which are within a few seconds into singular ones). By plotting these periods they attempt to graphically demonstrate the average period spacing, giving a result of 18 seconds. In the analyses, while taking into consideration the previous article, they state that this spacing is too small for the wave number to be $l = 1$, and must therefore be $l = 2$. A few problems arise when considering this method, first of all the combining of pulsations observed in different years whose periods are numerically close is hard to justify. The most accurate method would be to attempt to analyse data which is contained within each observation mission. The second important problem is that so as to get this result the assumption used for the graphical method is that all of the modes determined during the

observation missions from 1991 to 1999 be consecutive. This assumption is not one that we can take lightly, and seems a little far fetched.

Due to the rather optimistic requirements of Kanaan et al. (2000) so as to obtain the result that $l = 2$, this value will not be used. Instead the data presented here will adhere to the next best assumption on the value of the wave number (l), those based on the restrictions presented in Nitta et al. (2000), therefore all data on the pulsations of BPM 37093 presented in this paper will be for both the case of $l = 1$ and $l = 2$.

4.3 Convection

One of the problems in asteroseismology is the treatment of convection and its interactions with the pulsations of the star. As most DA white dwarf models up to date have used, the convection here will be dealt with using the mixing-length theory, which states that all rising and falling convective cells will travel one mixing length (l) before dissolving and exchanging its heat into the ambient medium. As discussed in Bergeron et al. (1992) the convective flux within the context of the mixing-length theory can be expressed by:

$$F_c = \frac{bC_p T l^2 \rho}{H_p} \left(\frac{agQ}{H_p}\right)^{\frac{1}{2}} (\nabla - \nabla')^{\frac{3}{2}} \tag{4.1}$$

where $(\nabla - \nabla')$ can be equated from

$$(\nabla - \nabla')^{\frac{1}{2}} = -\frac{B}{2} + \left(\frac{B^2}{4} + \nabla - \nabla_{ad}\right)^{\frac{1}{2}} \tag{4.2}$$

with B given by

$$B = \frac{\sigma T^3 d}{\rho l \tau_e C_p} \left(\frac{H_p}{agQ}\right)^{\frac{1}{2}} \tag{4.3}$$

where $\tau_e = \kappa l \rho$ is the optical depth of the convective cell and for optically thin convective cells

$$d = \frac{8\tau_e^2}{1 + \left(\frac{8\tau_e^2}{c}\right)} \tag{4.4}$$

The meaning of all of the different symbols can be found in the above article, those important in this discussion are the mixing-length (l), the local pressure scale height of the star's atmosphere (H_p), and the numerical constants; a, b, and c, which convey the efficiency of the convection. Based on different values of these three numerical constants, specific versions of the mixing-length theory can be identified. The three principle versions used in the context of white dwarf stars are presented in table 4.1.

Mixing length theory	a	b	c	$\alpha = l/H_p$
ML1	1/8	1/2	24	1
ML2	1	2	16	1
ML3	1	2	16	2

TABLE 4.1 – Version of the mixing length theory which are to be used

The convective efficiency of the ML2 version is greater then that of ML1, due to the fact that its parameters impose a reduced loss in energy during transport of the matter. The ML3 version is the same as ML2 only with $\alpha = l/H_p = 2$ causing this version to be the most efficient of all those presented here. A general rule is that the convective efficiency increases with increasing mixing-length version number.

By applying these three different versions of the mixing-length theory to different stellar models, an analysis of the effects of varying this parameter to the pulsations can be done. For these models the standard values of the stellar parameters of BPM 37093 were used, i.e.: $T_{eff} = 11730K$, $\log g = 8.81$, $\log q(H) = -4$ and $\log q(He) = -2$. The only other parameter required is the chemical composition of the core, and for analysis purposes as long as it remains constant throughout the study, this should not cause any variations in the results. As an arbitrary selection all of the models used here have cores composed of pure carbon (analysis of the effects of the chemical composition of the core is demonstrated later in section 4.4). After the pulsation code was applied to these static models it was possible to create graphs of the calculated period spectrum of the models as a function of the mixing-length theory used. Each of the curves in these period spectra represents a specific value of the radial order k, where the first curve at the bottom corresponds to the $k = 1$ radial order and the other ones increasing with consecutive k values. The graphs for the pulsations with wave

number $l = 1$ are seen at the top of figure 4.1, while the pulsations of $l = 2$ wave number are shown at the bottom. When analyzing the graphs it is important to keep in mind that even though the period spectrum represented is from 0 to 1000 seconds, the observed pulsations for BPM 37093as presented in table 3.1 , have periods within 500 to 650 seconds, so this region is the most important.

Figure 4.1 confirms prediction 11 from Brassard et al. (1992a) (seen in table 2.1), that the period of individual modes increase as the convective efficiency is increased. The variation is detectable but is rather small compared to the scale of the whole system. The average period spacing between consecutive radial overtones for the pulsations with periods between 500-650 seconds, has been calculated for the three convective efficiencies and is presented in table 4.2. These are in accordance with prediction 3 presented in table 2.1.

Mixing length theory	$<\Delta$Period$>$(s) for $l = 1$	$<\Delta$Period$>$(s) for $l = 2$
ML1	20.7481	12.2418
ML2	21.4203	12.7963
ML3	21.9314	12.9233

TABLE 4.2 – the average change in period ($< \Delta P >$) of the models created with the 3 mixing-length theory version for each values of l

Varying the convective efficiency has no large effects on the pulsation periods, overall change to the average period spacing for pulsations with wave number $l = 1$, caused by using ML3 instead of ML1 is approximately 1.2 seconds. This is very small considering the overall scheme of the model studied here. This effect represents a physical situation in which the relaxation time of the material which is moved through convection is so short that it can respond to pulsations right away. This is also noted in (Fontaine et al. 2003b) which states that, the convective flux in a DA adjusts instantly to the perturbations caused by convection. Therefore no matter how effective the convection theory is there is little change to the pulsations of the system, thus making the convective theory used a very small source of uncertainty in the comparison of the pulsations created for the model to the observed variations. For the models calculated hereafter the mixing length theory that will be used will be ML2.

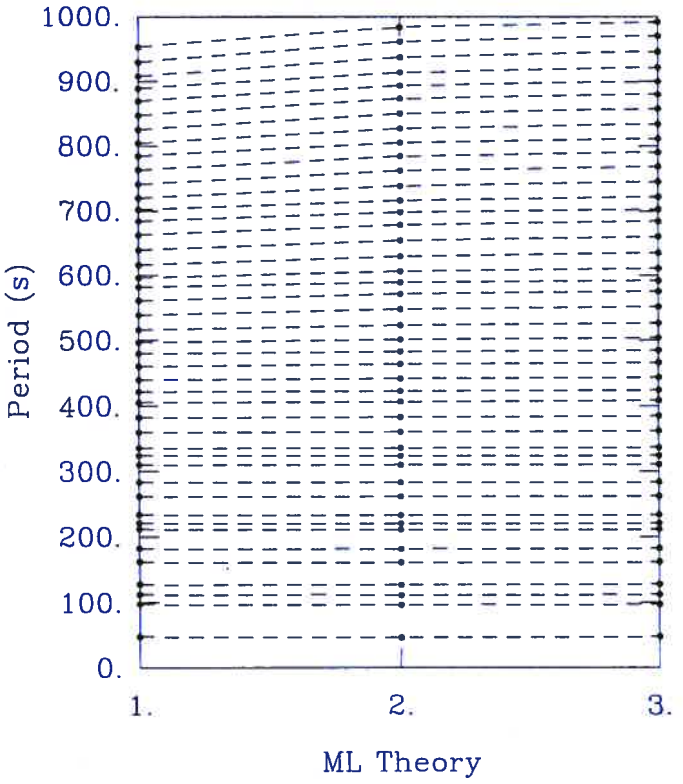

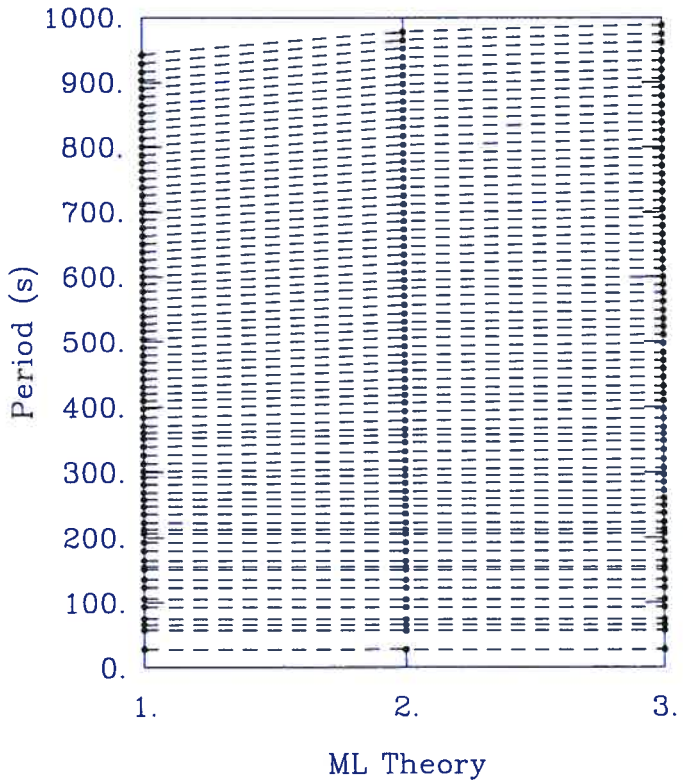

FIGURE 4.1 – Convective efficiency vs. the period of pulsations for a 100% Carbon model with $l = 1$ above and $l = 2$ below. Here the versions of the mixing-length theory are represented as follows: 1 stands for ML1, 2 for ML2 and 3 for ML3

4.4 Core Composition

From accepted theoretical models of white dwarfs we can safely assume that the chemical composition of the core of BPM 37093 is a mix of only two elements, carbon and oxygen, but the actual ratio of abundance is unknown. So as to be able to determine if the chemical composition of the models has an effect on the pulsations, a comparison of the different possible chemical configurations was required.

All of the models which will be discussed have the standard values for the variables of pulsation of BPM 37093 (as seen in chapter 3), and only the fraction of crystallization of the star (M_{xtal}/M_*) will be varied. The reason for using the fraction of crystallization as the independent parameter is this situation, and the use of only the pulsations with wave number $l = 1$ is based solely on the fact that this specific configuration creates enough spacing between consecutive modes so that the effects of changing the core composition can clearly be studied without any interference of adjacent modes. The effects of varying the fraction of crystallization will be examined further on in this paper and is not the purpose of this section.

Figures 4.2 and 4.3 are graphical representation of the effects of varying the chemical composition of the stellar core. In figure 4.2 we are comparing the period spectrum created from a model with a core composition of pure carbon (solid line) vs. the period spectrum representing a model with the core of exactly half carbon and half oxygen (the dotted line), while in figure 4.3, the two models being compared have cores composed of pure carbon (solid line) and pure oxygen (dotted line). As we can see in the first figure and more prominently in the second, the curves of the individual k modes do not overlap perfectly for all of the values of M_{xtal}/M_*. Within our region of interest, (500-650 seconds) in particular the situation seems to be the most organized, with same k mode curves of the two core compositions sharing the same form only with a shift towards the lower crystallization fraction as the ratio of oxygen to carbon in the core is increased. This effect causes the difference of the two curves to be more prominent in figure 4.3 than it is in 4.2 since there is a greater difference in the quantity of oxygen found within the core of the two compared models.

For a closer view of this effect figure 4.4 shows the two $k = 23$ mode curves from figure 4.3 isolated from the others. Here the curves resemble steps, with the period of each of the

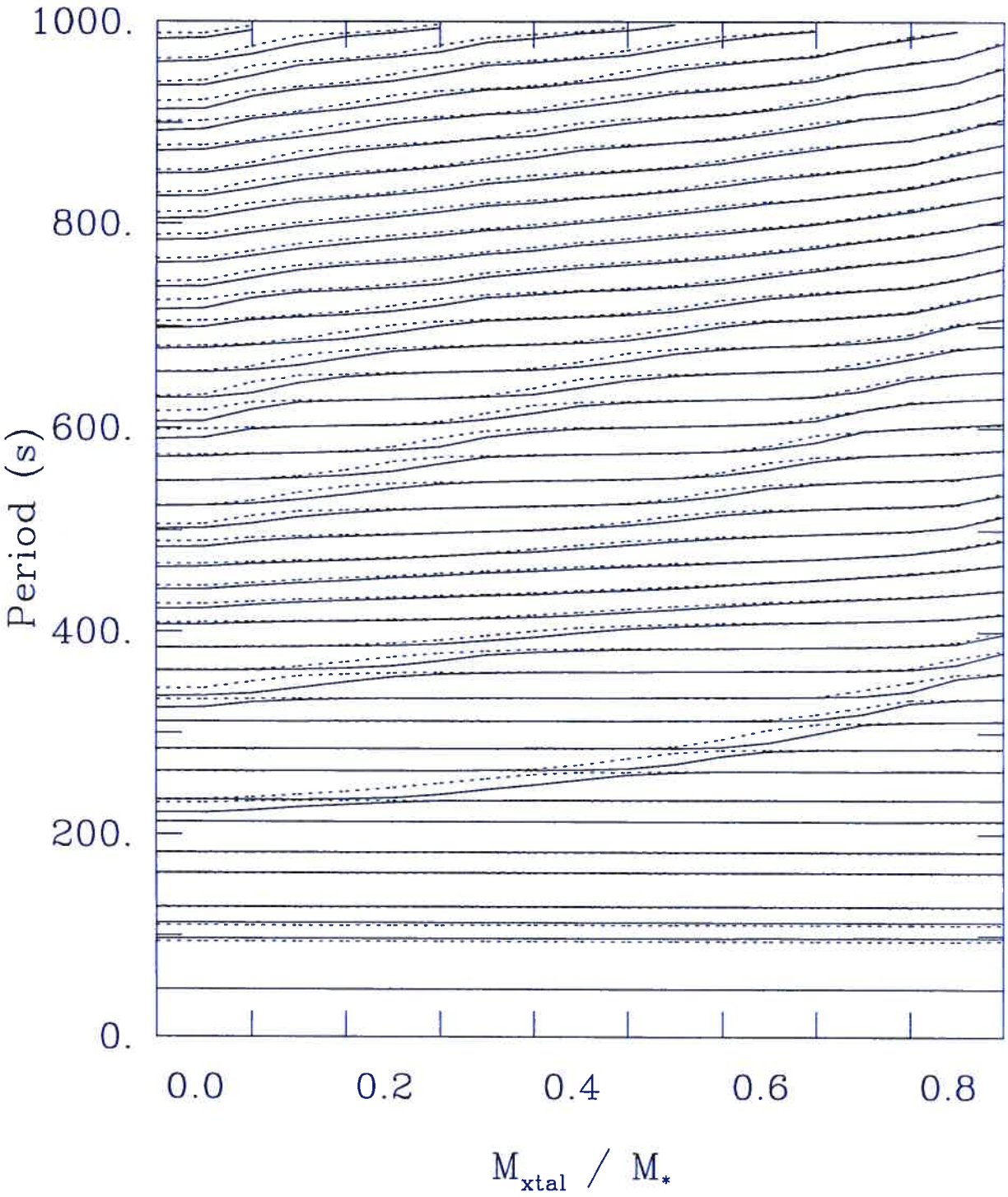

FIGURE 4.2 – Fraction of crystallization vs. period for both the model with 100% Carbon core (the solid line) and the model with 50% Carbon and 50% Oxygen model (the dotted line), with $l = 1$.

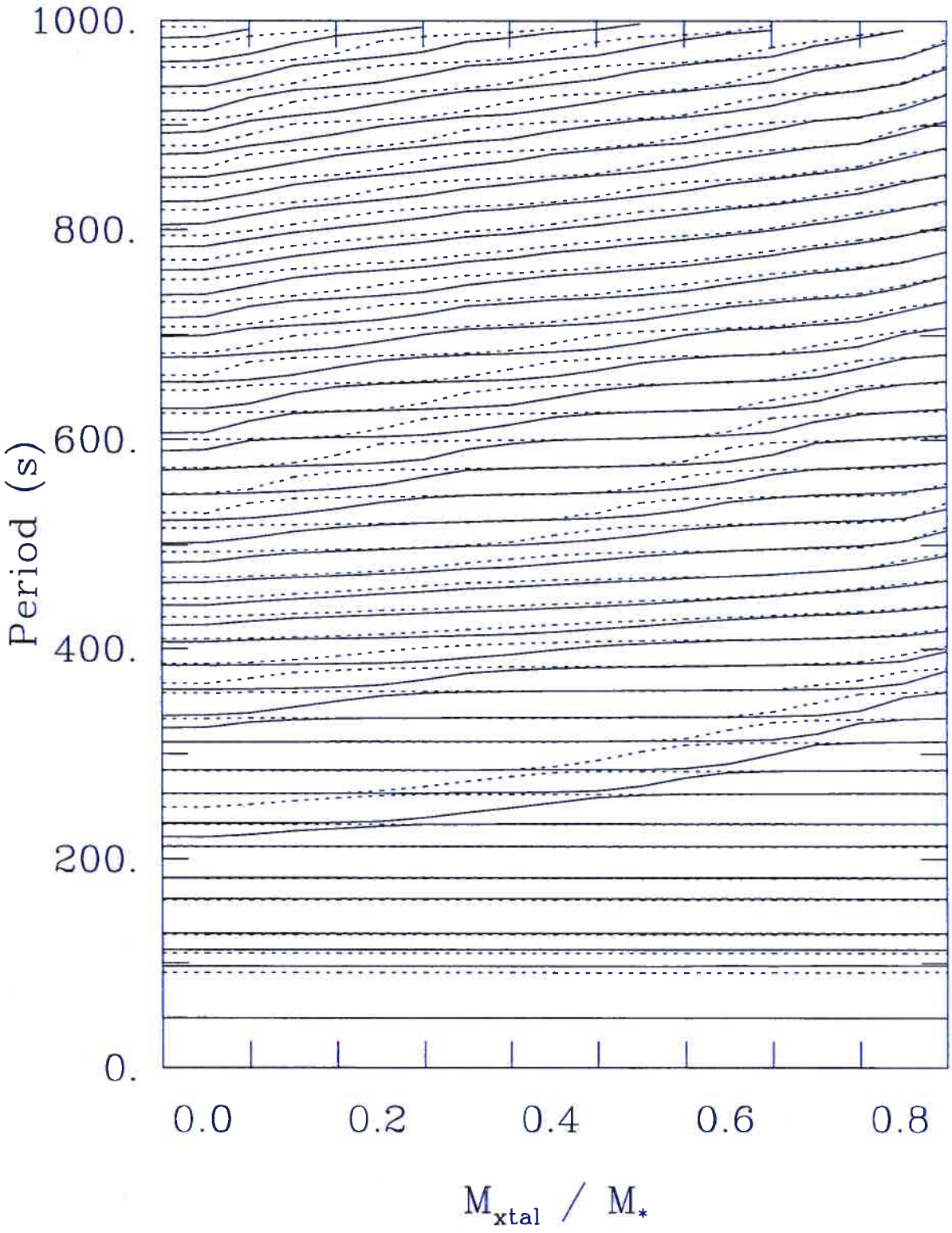

FIGURE 4.3 – Fraction of Crystallization vs. period for both the model with 100% Carbon core (the solid line) and the model with 100% Oxygen model (the dotted line), with $l = 1$.

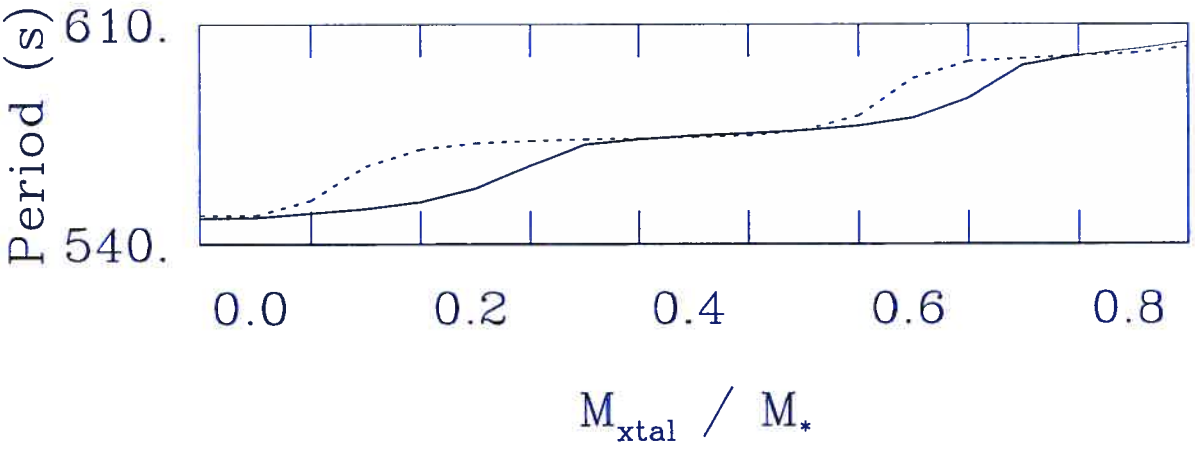

FIGURE 4.4 – Fraction of Crystallization vs. the period of the $k = 23$ lines for both the model with 100% Carbon core (the solid line) and the model with 100% Oxygen model (the dotted line), with $l = 1$.

modes rising to a specific value and then creating a plateau. Especially of note here is the fact that model with the oxygen core achieves these plateaus at smaller values of the fraction of crystallization, while the two curves seem practically identical. Therefore the innate variation caused to the pulsations due to a changing the core composition is unmistakable, if only small.

As a proof that these effects are solely based on the chemical composition the same procedure as above was followed only this time the thickness of the hydrogen layer is used as the independent variable and the crystallization is set to 0%. Figure 4.5 shows the $k = 22$ modes for two models, one with a core composed of only carbon (solid line) and the other of pure oxygen (dashed line). Here again there is a shift of the curve towards a smaller variation of the independent variable as the amount of oxygen in the core is increased. Due to the nature of the curves created when the $\log q(H)$ is varied (as seen later in section 4.8), the ordered steps seen in the figures involving the fraction of crystallization are stretched almost beyond recognition.

As seen in section 2.2.4 pulsations of a star are affected by the interaction of two areas with different chemical compositions based on the calculated Brunt-Väisälä frequency. In this calculation the B factor represents the location where the trapping of the modes occurs, and is directly dependant on the chemical compositions of the two areas that are coming into contact

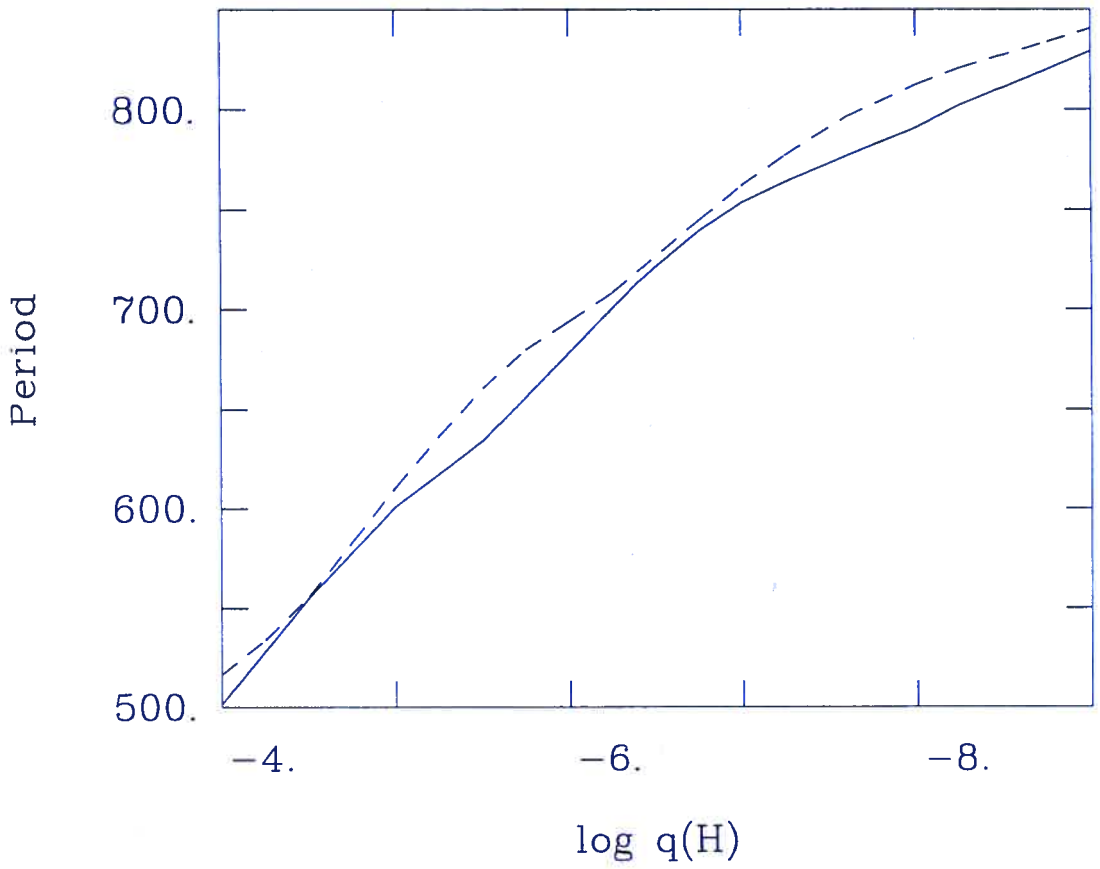

FIGURE 4.5 – Thickness of the Hydrogen layer ($\log q(H)$) vs. period of the $k = 22$ lines for both the model with 100% Carbon core (the solid line) and the model with 100% Oxygen model (the dotted line), with $l = 1$.

at this transition zone. Within DAVs there are two main chemical transition zones to consider; first is the outermost transition zone where the hydrogen layer which is found around the rest of the star comes into contact with the helium zone directly within it, and secondly the innermost transition zone of the helium layer with the core. For this study due to the fact that the only chemical change occurring between the compared models is within the core, the B factor which is representative of this Hydrogen-Helium interaction will be the same in both models, and therefore the outermost transition zone will not contribute to the differences observed in the calculated period spectra above. These variations will therefore only be dependent on the transition zone of the helium layer with the core of the star. Since half of the situation in both models is the same, there is an interaction of some chemical composition with a pure hydrogen layer, the differences arise from the contribution of the chemical composition of the core to the B factor of the Brunt-Väisälä frequency. This difference in core composition will cause the mode trapping to occur at different locations and therefore cause the pulsations to change.

Now that it has been determined that the variation in the chemical composition of the core does in fact create changes in the pulsations, it is important to know if these changes are important ones for our stellar model. So as to verify this the average period spacings between consecutive modes ($< \Delta P >=< P_{k+1} - P_k >$) of the pulsations with periods within 500-1000 seconds, for the three main core compositions are graphically represented as factors of the crystallized fraction in figure 4.6. The pulsations with $l = 1$ and $l = 2$ wave numbers are found in two distinct, and very tight groups, with the first group being above the latter. Within the groups we have the pulsations created for the models of all three of the chemical compositions, that of pure carbon, pure oxygen, and a model with an exact mixture of the two. From this it can easily be seen that the actual effect of changing the chemical composition of the core has little effect on the average period spacing. Therefore even though there is a shift in the pulsation curves when the core composition is changed, the overall effect to the average period spacing is almost nil, so the chemical composition of the core should not factor in greatly to the pulsations created numerically for any of the models.

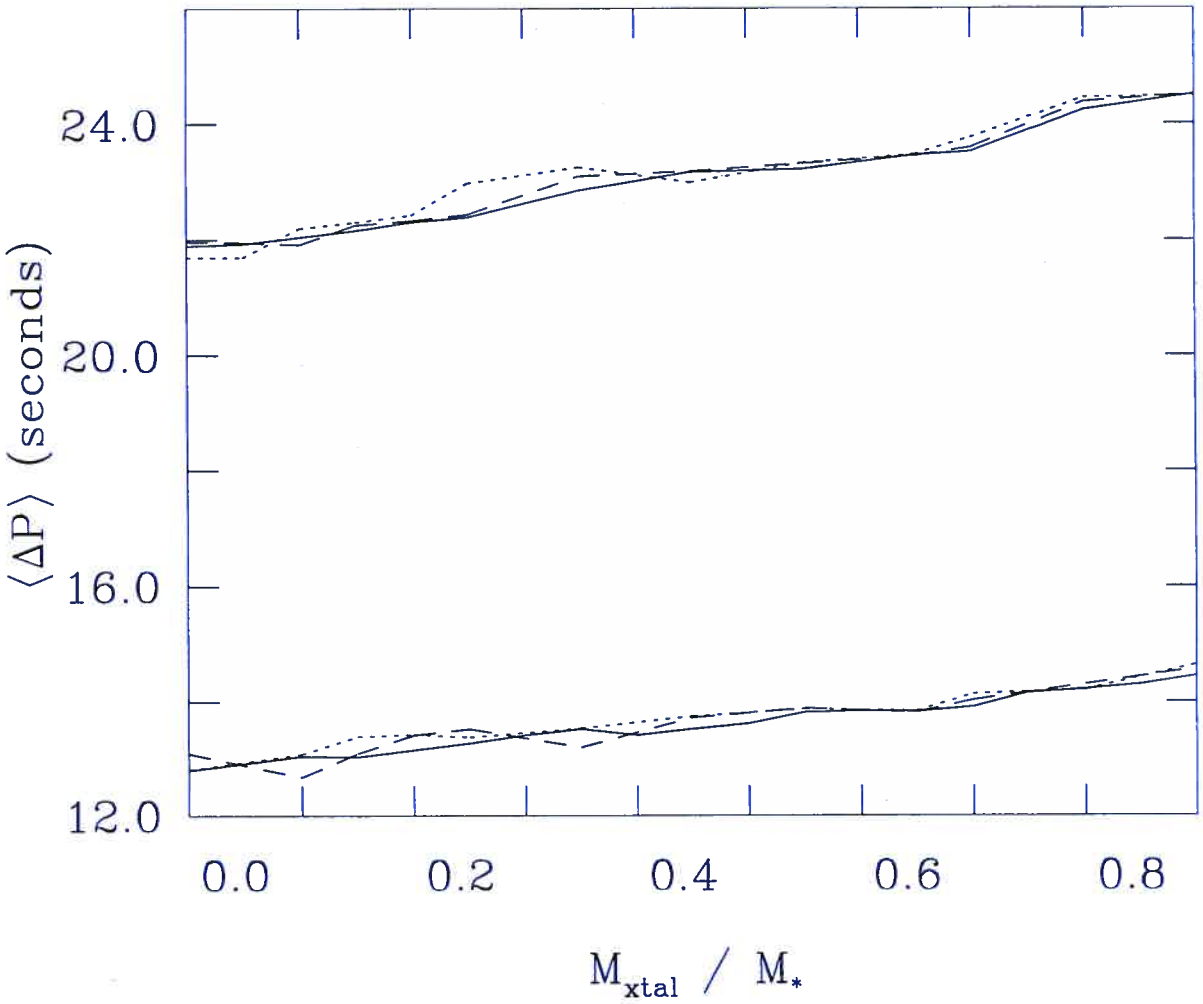

FIGURE 4.6 – The plots of the average period spacing ($< \Delta P >$), for pulsations with periods limited within 500-1000 seconds, versus the fraction of crystallization of the star (M_{xtal}/M_*). The above and below collections of curves represent the pulsations within the $l = 1$ and the $l = 2$ wave number groups respectively. The two solid lines represent the model with a pure carbon core, the dotted lines represent the model with a core composed of pure oxygen, and the dashed lines represent the model with a mixed core of equal parts oxygen and carbon.

4.5 Effective Temperature (T_{eff})

As seen in section 3.1 the effective temperature of BPM 37093 has a determined value of $11730 \pm 200K$. For a temperature of this magnitude an uncertainty of only $200K$ (as determined in Fontaine et al. (2003a)) is very small, allowing the possibility that the impact on the pulsations of varying this parameter throughout it's allowed range will also be small. The overall effects which should be seen as the effective temperature is increased, as discussed in Brassard et al. (1992a) (presented in this paper in table 2.1), are the decrease of both the period of the individual k modes and the average period spacing between two consecutive modes which have the same wave number l.

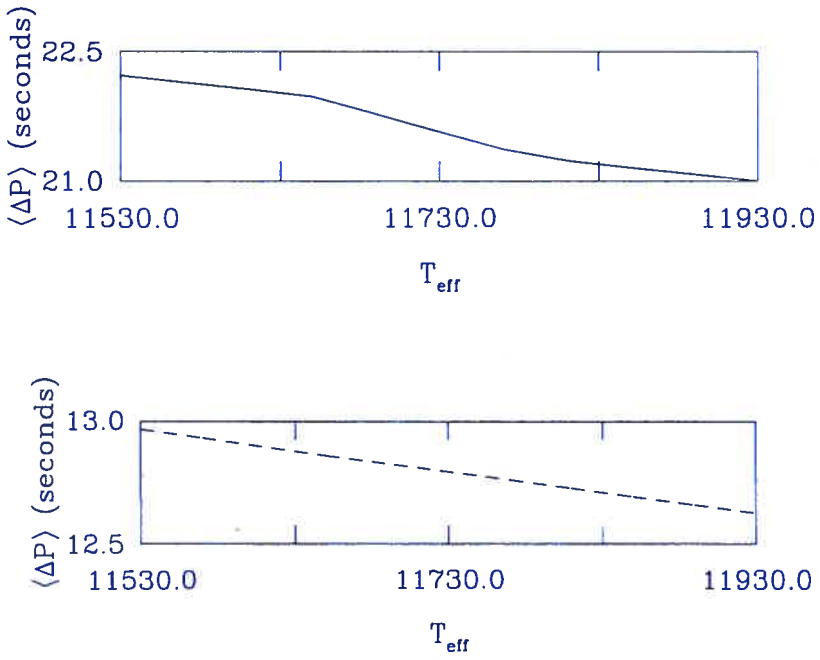

FIGURE 4.7 – Effective temperature versus the average period spacing. Pulsations with $l = 1$ are shown above, and below is for those with $l = 2$

In figure 4.7 the average period spacing between consecutive modes of pulsations with periods between 500-1000 seconds is plotted versus the effective temperature for models in which the core composition is pure carbon, where the upper graph represents the pulsations with wave number $l = 1$, while the lower graph is for the those with $l = 2$. The average period spacing in these calculations does in fact decrease as the temperature increases but

this change is so small that the difference between the upper and lower limit of the given temperature range is within 1.5 seconds for both values of the wave number. This is a very small change indeed when compared to the overall system.

For figure 4.8 the calculated period spectrums of the $l = 1$ (above) and $l = 2$ (below) wave number pulsations are in accordance with the predictions, showing a decline in the periods of each individual pulsation mode (k value) as the effective temperature is raised. This change though is very small, and is almost nil within the 500-650 second period limit of the pulsations observed in BPM 37093.

Varying the effective temperature within this very small margin of error imposes very little changes to the calculated pulsations, so small that they can almost be considered as nil. Therefore unless all of the other parameters of pulsation have effects that are as minuscule as this one, the effective temperature will not be considered as one of the major contributors of uncertainty to the pulsations of BPM 37093.

4.6 Surface gravity ($\log g$)

Along with the effective temperature of a star, another major physical parameter that can be determined through observation is its mass. As discussed in section 3.2, when modeling stars it is more effective to deal with the value of the surface gravity in the form $\log g$, then directly with the mass of the star, and for BPM 37093 the value of this parameter is known to be $\log g = 8.81 \pm 0.05$. Much as in the case of the effective temperature the margin of error is very small relative to the parameter itself, this is again due to the accuracy of the optical spectroscopy approach, as discussed in Fontaine et al. (2003a). The small ratio of the margin of error to the $\log g$ might again create a situation in which the variation of this parameter will have little effect to the pulsations created for these models, and to verify this an overview of the situation needed to be done.

The expected results of increasing the value of the surface gravity would be to decrease both the period of each individual pulsation modes and the average period spacing between consecutive modes (from Brassard et al. (1992a) presented in table 2.1). Physically this can be explained due to the fact that increasing the value of $\log g$ is directly proportional to increasing

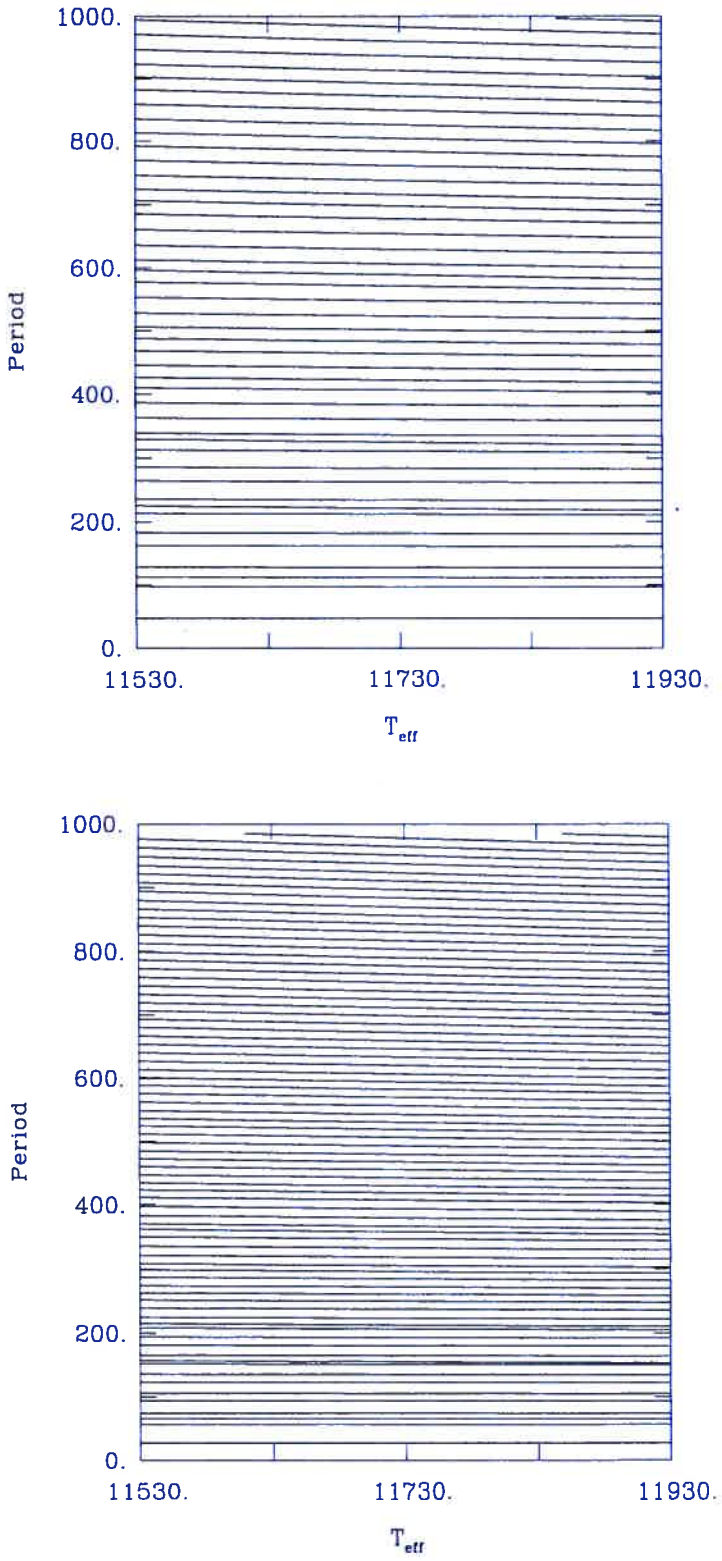

FIGURE 4.8 – Effective temperature vs. the period for the pulsations present on a model with a core composition of half oxygen and half carbon. The graph at the top is for the pulsations with l=1, while the one below is for those with l=2

the mass of the model, and within white dwarfs this also causes a decrease in the radius. With this increased mass and decreased radius the density is augmented forcing smaller periods for the individual pulsations as well as decreasing the separation between consecutive pulsations. So as to determine if in fact these two phenomena are occurring within our created system we examine figure 4.9 which charts the effects that varying the $\log g$ has to the calculated period of the pulsations. Represented here are both the $l = 1$ (upper section of the figure) and $l = 2$ (lower section) wave number pulsations of a model with a core composition of exactly half oxygen and half carbon.

In both of the calculated pulsation models of figure 4.9 we do in fact see the expected effects of varying the input parameter, there is a definite tendency present in all of the curves to decrease in period as the value of the $\log g$ if increased, and this effect is more prominent then that observed in the models involving the variation of the effective temperature. Not as obvious in this figure is the effect of varying this parameter upon the average period spacing, for this analysis we must examine figure 4.10. This is a graph of the average period spacing, for pulsations with periods within 500-1000 seconds, plotted versus the variation of the surface gravity. It can be seen from this figure that for the pulsations of wave number $l = 1$ and $l = 2$ the average period spacing decreases as the value of the surface gravity is increased, as anticipated. It should be noted that even though the effect here is larger than that observed within the context of the effective temperature, overall it is still rather small. For the $l = 1$ pulsations the average period spacing only varies within 3 seconds from one end of the $\log g$ spectrum to the other, and the range is even smaller for the $l = 2$ pulsations.

Overall we see that the effects of varying the value of the surface gravity do in fact coincide with the expected results, and as speculated before, due to the relatively small margin of error, these effects were appropriately small. Though having a greater effect than the effective temperature, it is still most likely that in the end the uncertainty that is present on the value of the surface gravity will not contribute much as a source of uncertainty for the modellization of the variability of BPM 37093.

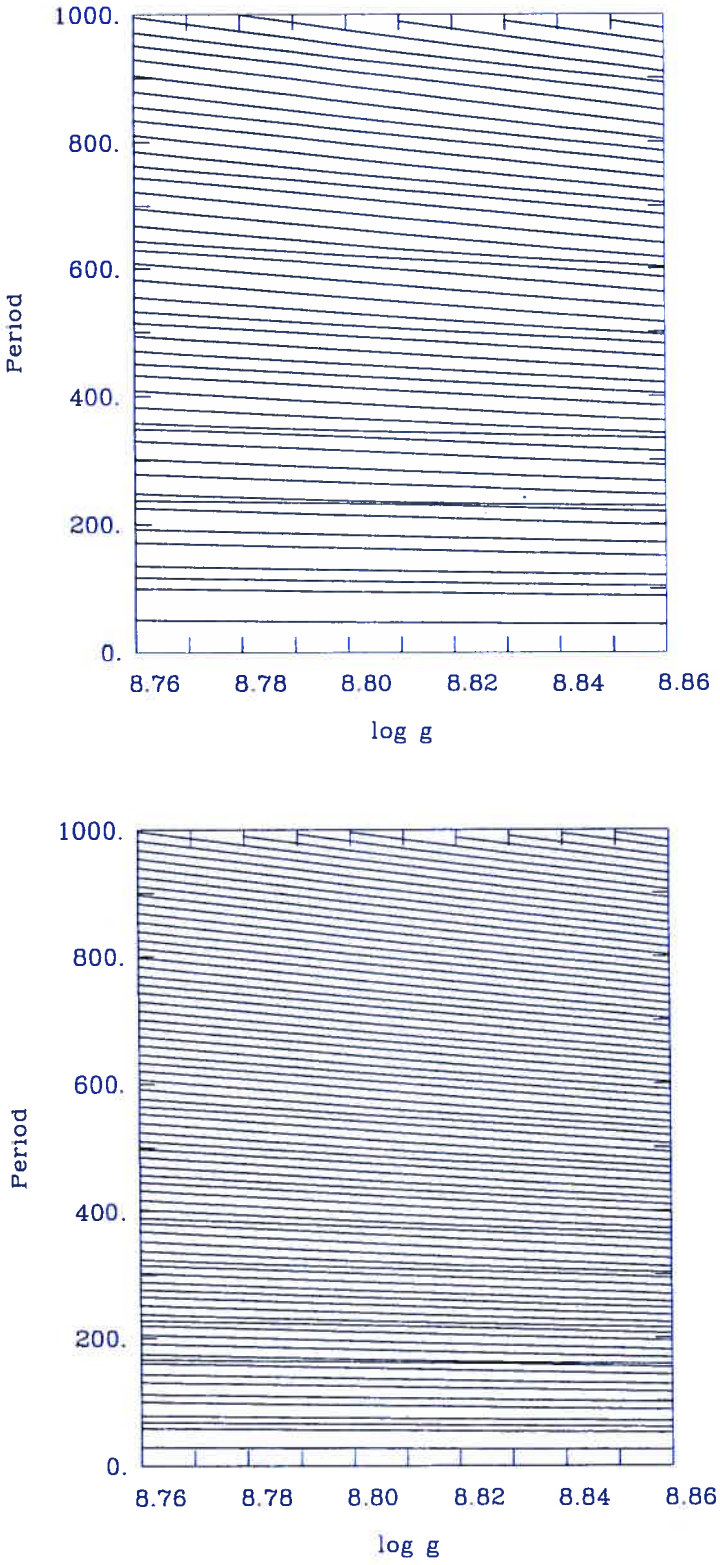

FIGURE 4.9 – Surface gravity ($\log g$) vs. Period for a model with a core composition of exactly half carbon and oxygen. Here the pulsations with wave number $l = 1$ are on the top and $l = 2$ on the bottom

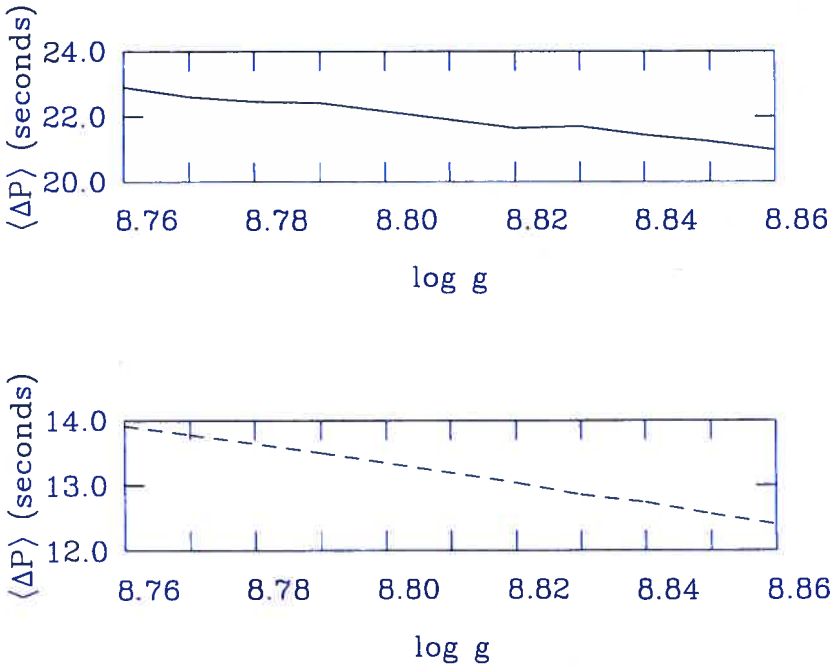

FIGURE 4.10 – Surface gravity vs. the average period spacing ($< \Delta P >$). Both graphs are for a model with a core of half carbon and half oxygen, with the above for pulsations with $l = 1$ and below for those with $l = 2$

4.7 Thickness of the Helium layer ($\log q(He)$)

The thickness of the helium layer represented as $\log q(He)$ (as calculated from equation 3.2), is actually referring to the mass of the inner helium layer of the star, and from the structure of BPM 37093 this parameter is confined to a region $-4 \leq \log q(He) \leq -2$ (discussed in section 3.3). For this analysis the non-varying parameters will have the same standard values as those proposed throughout this research, $T_{eff} = 11,730K$, and $\log g = 8.81$, the only exception to this standard model is the representation of the thickness of the hydrogen layer which will have a value of $\log q(H) = -6$. This difference from the standard value is due to the range of $\log q(He)$ which will be used, and the physical coupling required between the hydrogen and helium layers of the star, as explained in chapter 3.

When the pulsation code was applied to a model created with the above parameters and with a core composition of half carbon and half oxygen, the calculated period spectrum created as a function of the thickness of the helium layer is seen in figure 4.11. From this we

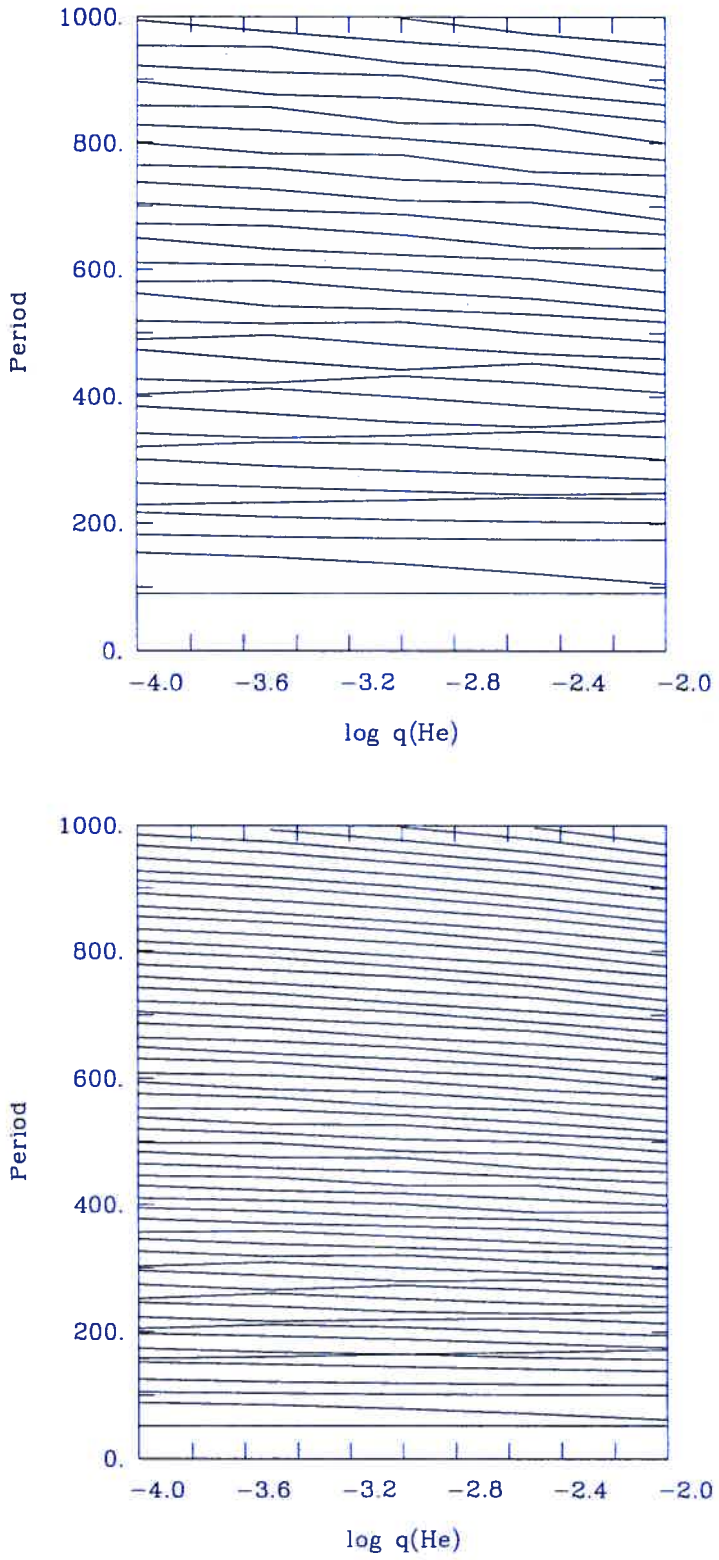

FIGURE 4.11 – $\log q(He)$ vs. period for both the $l = 1$ (top) and l=2 (bottom) pulsations of a model with a mixed core of equal parts carbon and oxygen

see that there seems to be a very small tendency to increase the period of each of the modes as the $\log q(He)$ is decreased, but the effect is extremely minimal. The more obvious effect of varying this parameter is to change the layout of the maximums and minimums present between consecutive modes, moving from one location in the parameter space to another in a smooth manner. This tendency is a representation of the phenomenon known as avoided crossing in which two modes approach and induce within each other "rapid shifts" of frequency (or period as seen here), an in-depth discussion of the phenomenon is presented in Aizenman et al. (1977). The general effect of separation of the two modes occurs so as to prevent them from sharing the same frequency. An application of this to the whole system causes these locations of distinct maxima and minima, as seen in figure 4.11. Though the average period spacing seems to change a great deal within these areas, a graphical representation as in figure 4.12 of this mean change to the periods needs to be analyzed more closely so as to demonstrate the real effects.

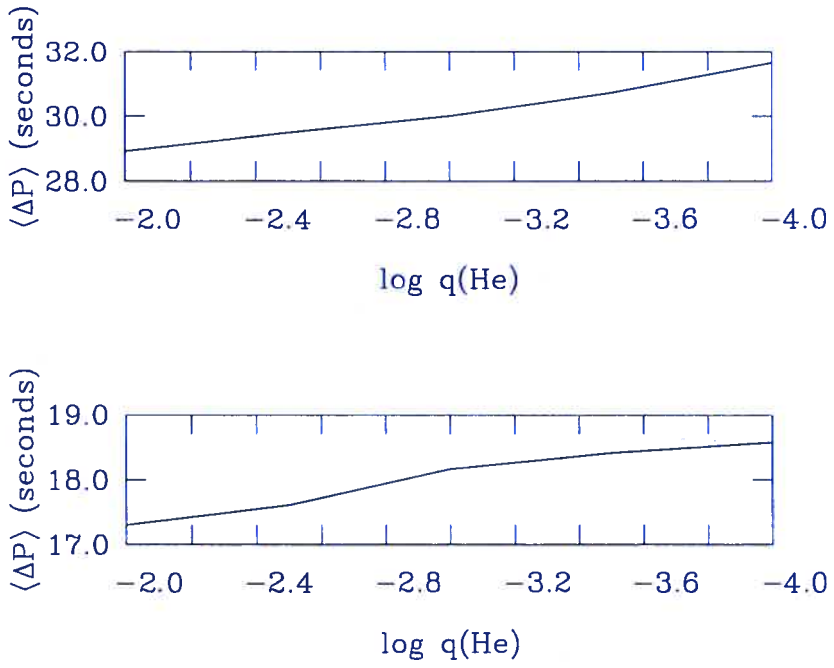

FIGURE 4.12 – $\log q(He)$ vs. the average period spacing for a model with a core composition of half carbon and half oxygen, with $l = 1$ on the top and l=2 on the bottom. All of the pulsations included within the calculation of these mean values have periods falling within 500-1000 seconds

The upper section of figure 4.12 represents the pulsations with $l = 1$ wave number, within the range of periods from $500 - 1000$ seconds. Here the effect to these usually rather sensitive pulsations is only a change to the period of less than three seconds, as the parameter is varied from one extreme to the other of its allowed range. The same is also true for the $l = 2$ curves (bottom of figure 4.12) which only show an overall change within one and a half seconds from one extreme to the other of the allowed parameter space. This is a very small shift in the period when considering that this is due to a shift of $\log q(He)$ from -2 to -4, the full extent studied.

When the thickness of the helium layer is changed much activity is created within the period spectrum, as seen in figure 4.11. Most of this activity is in the form of the moving of the maxima and minima between consecutive modes due to the phenomenon of avoided crossing. Though these effects individually seem to be very large and the pulsations themselves are affected on a larger scale then what has been seen so far, the average period spacing of the system as a whole, as was seen in figure 4.12, remains small. Thus far the thickness of the helium layer can be categorized as the most important source of variation in the calculated pulsations of the system. Still the variation of this parameter within the physical limits imposed by the theory has rather small effects to the pulsations created in the numerical model when considering the system as a whole. Unless all of the remaining parameters are as ineffective in driving variations in the pulsations as those studied so far, it is still rather unlikely that the thickness of the helium layer will play a major part in the creation of uncertainty in the modellization of the physical processes at work within BPM 37093.

4.8 Thickness of the Hydrogen layer $(\log q(H))$

The last parameter whose effects on the pulsations will be compared to those caused by the crystallization of the star, is the thickness of the hydrogen layer. Much as with the helium layer, the hydrogen layer thickness can be represented as $\log q(H)$, in accord with equation 3.1. With the information presented in section 3.3 on the theory behind this parameter, it is known that the value falls within the range of $-4 \leq \log q(H) \leq -9$. So as to determine the effects of varying this parameter within the allowed range, the pulsations of the system with

different values of $\log q(H)$ needed to be calculated. The expected results of such variation as expressed in table 2.1, were that as the thickness of the hydrogen layer was decreased both the average period spacing between adjacent modes and the periods of each individual modes would increase. A demonstration of the latter situation is demonstrated in figures 4.13 and 4.14, that is plots of the period of individual modes versus the effects of changing the $\log q(H)$, both of these figures are representations of the numerical simulation of the pulsations created for a model with core composition of pure carbon. The only difference between the two figures is that the first demonstrates the pulsations with wave number $l = 1$, while the other figure is for the pulsations with $l = 2$ wave number.

It is obvious from both figures that the effects of the variation of $\log q(H)$ to the pulsations are huge. For some of the $l = 1$ curves the period increases by over 200 seconds as the thickness of the hydrogen layer is varied from one extreme to the other of its allowed range. This magnitude of difference was unheard of in the cases previously discussed for the other parameters of pulsation. For a clearer view of the situation figure 4.15 demonstrates the effects of the variation of $\log q(H)$ to the average period spacing ($< \Delta P >$) between the consecutive pulsations with periods in the range from 500-1000 seconds, of the same model as used above.

Again the amount of change caused by the variation of this parameter is enormous, dwarfing all of the differences caused by the previously discussed parameters. As an example the difference imposed to the average period spacing by a change of $\log q(H)$ from -4 to -5 only, is on the order of 4 seconds for the $l = 1$ pulsations. This difference alone is larger then any demonstrated for the other parameters when they were varied from one extreme to the other of their allowed uncertainty ranges. Obviously this parameter is the dominant cause of variation in the pulsations from all of the ones discussed so far. Even if the value of this parameter which is used in simulations is only off by a small amount from the true value of the star, the resulting effect could be calculated pulsations which are very different from those actually present in BPM 37093. Thus this parameter is a very large source of uncertainty in the use of stellar pulsation models as a tool for asteroseismological studies of BPM 37093.

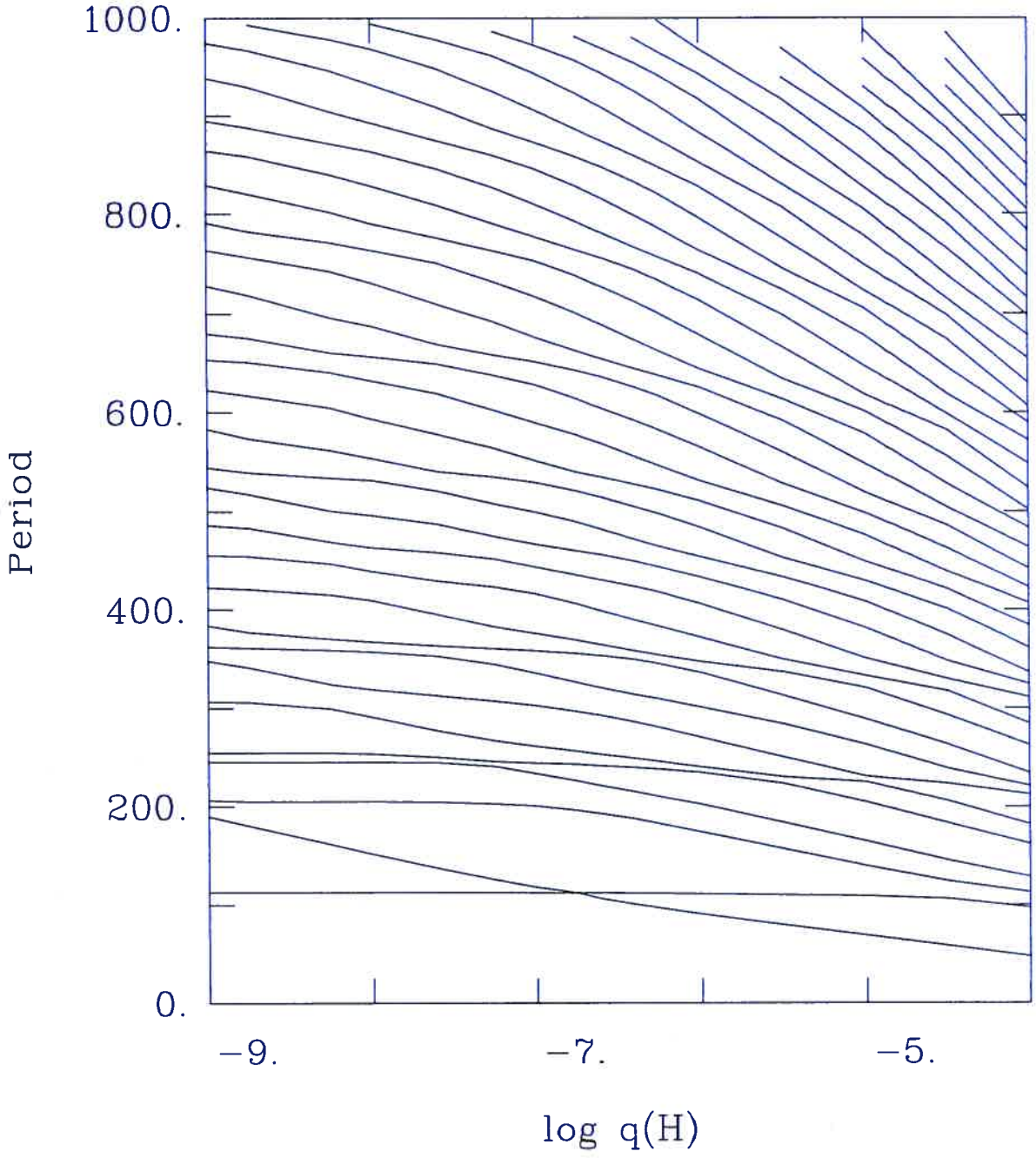

FIGURE 4.13 – Thickness of the Hydrogen layer ($\log q(H)$) vs. the period for the $l = 1$ pulsations of a model with a core composed of pure carbon.

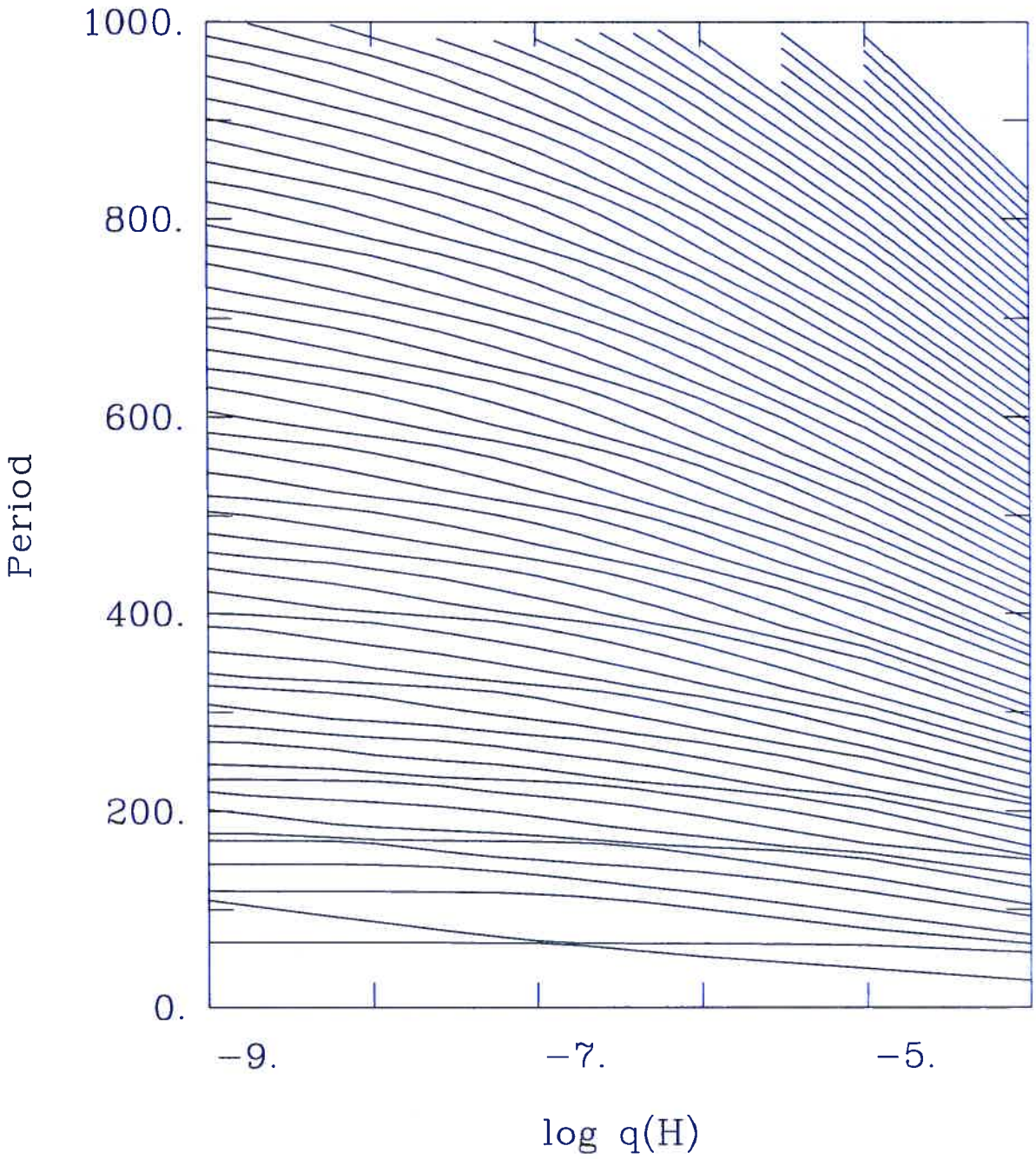

FIGURE 4.14 – Thickness of the Hydrogen layer ($\log q(H)$) vs. the period for the $l = 2$ pulsations of a model with a core composed of pure carbon.

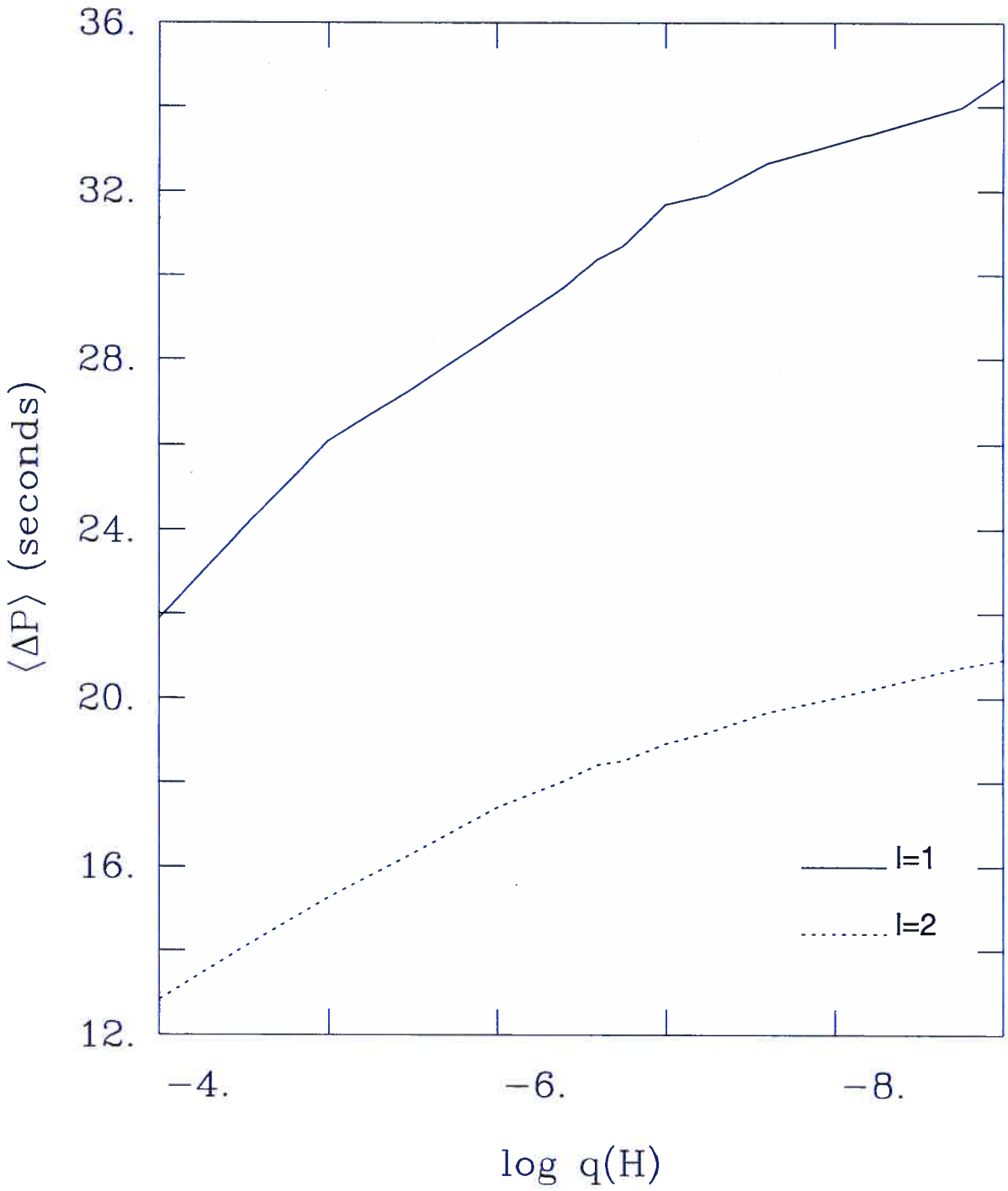

FIGURE 4.15 – $\log q(H)$ vs. the mean period spacing, $< \Delta P >$ for pulsations with periods within 500-1000 seconds, created for a model with a core composition of pure carbon. The two curves represent the pulsations with wave number; $l = 1$ for the line above and $l = 2$ for the line below

4.9 Crystallization

As mentioned throughout this paper and discussed in more detail in section 3.6, due to its high mass and our knowledge of cooling white dwarfs we know that BPM 37093 does in fact have a crystallized core. So as to be able to correctly simulate the effects that this crystallized core has to the pulsations within the star, the models created with the standard parameters needed to be truncated, thus allowing a numerical method to represent the fact that the interior regions would no longer be available to the propagation of pulsations. The location of the truncation of the data was determined by specific values of $\log q(H)$, as stipulated by equation 4.5.

$$\log q = \log\left[1 - M_{xtal}/M_*\right] \tag{4.5}$$

where M_{xtal}/M_* is the desired fraction of the star's mass which is crystallized, and for this research the range of $0.00 \leq M_{xtal}/M_* \leq 0.90$ is used, thus simulating models which are from 0 to 90% crystallized. The method of direct truncation of the models used here is an application of the hard-sphere boundary condition described in Montgomery & Winget (1999). This condition, whose validity is defended in the aforementioned article, simulates realistically the solid/liquid interface which occurs between the crystallized core which is unable to sustain the shear motions required to propagate the non-radial g-modes, and the outer layers of the star. After these models were created and truncated at the correct location the pulsation code was applied so that the effects could be determined. The model presented here is one in which the core is pure carbon, with the values of the other parameters of pulsation remaining standard.

It is obvious in figure 4.16 and figure 4.17 that the crystallization does in fact have an effect on the period of the pulsations present, as the stellar fraction of crystallization is increased so to does the period of the individual modes. For a $l = 1$ pulsation within the desired period range for the star, it increases by approximately 50 seconds as the fraction of the star which is crystallized is increased from 0% to 90%. Within this same range of 500-1000 seconds the average period spacing between consecutive modes can be seen in figure 4.18. Here the solid

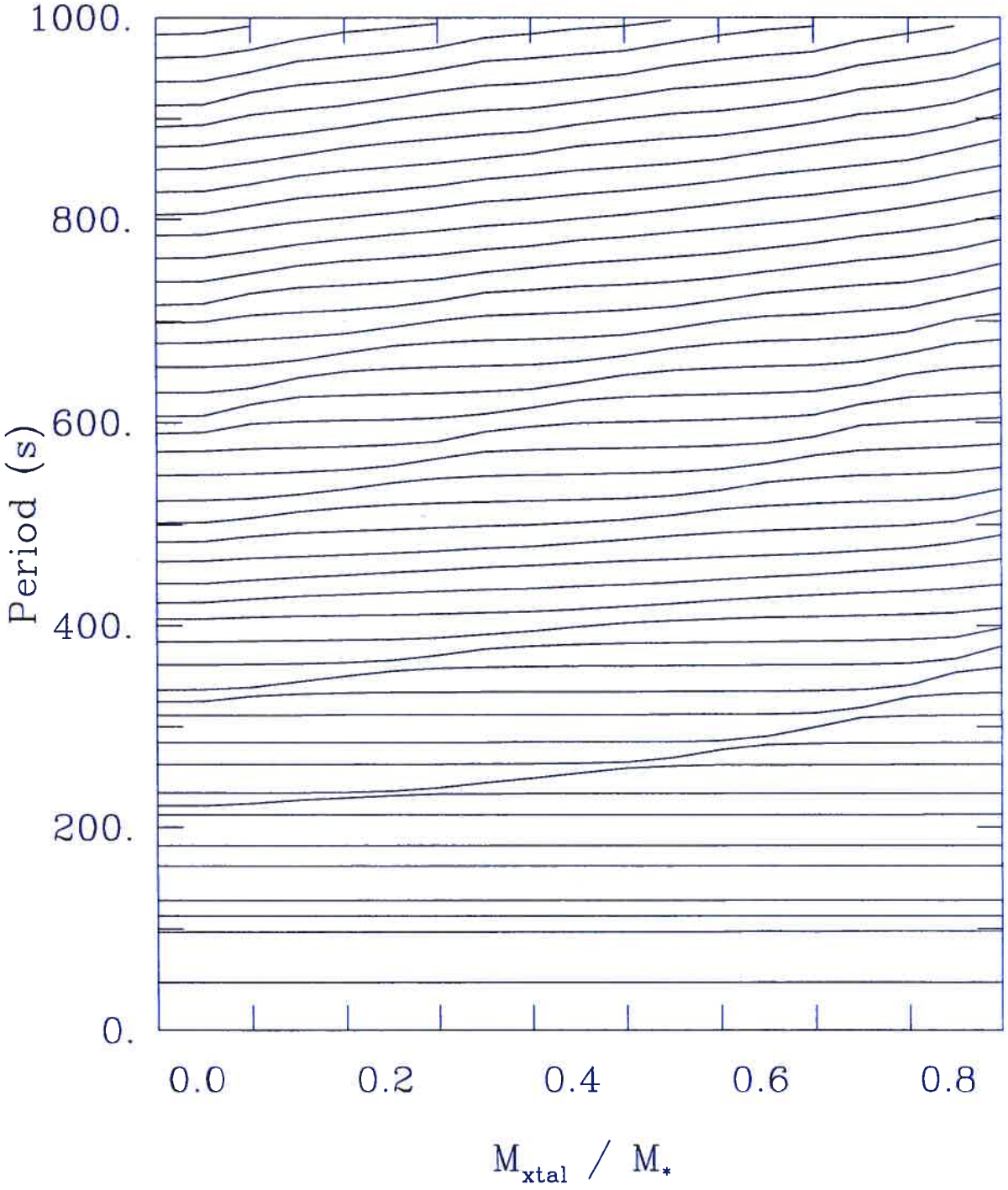

FIGURE 4.16 – Fraction of crystallization (M_{xtal}/M_*) of a model with a core composed of pure carbon vs. the period of the pulsations with wave number $l = 1$.

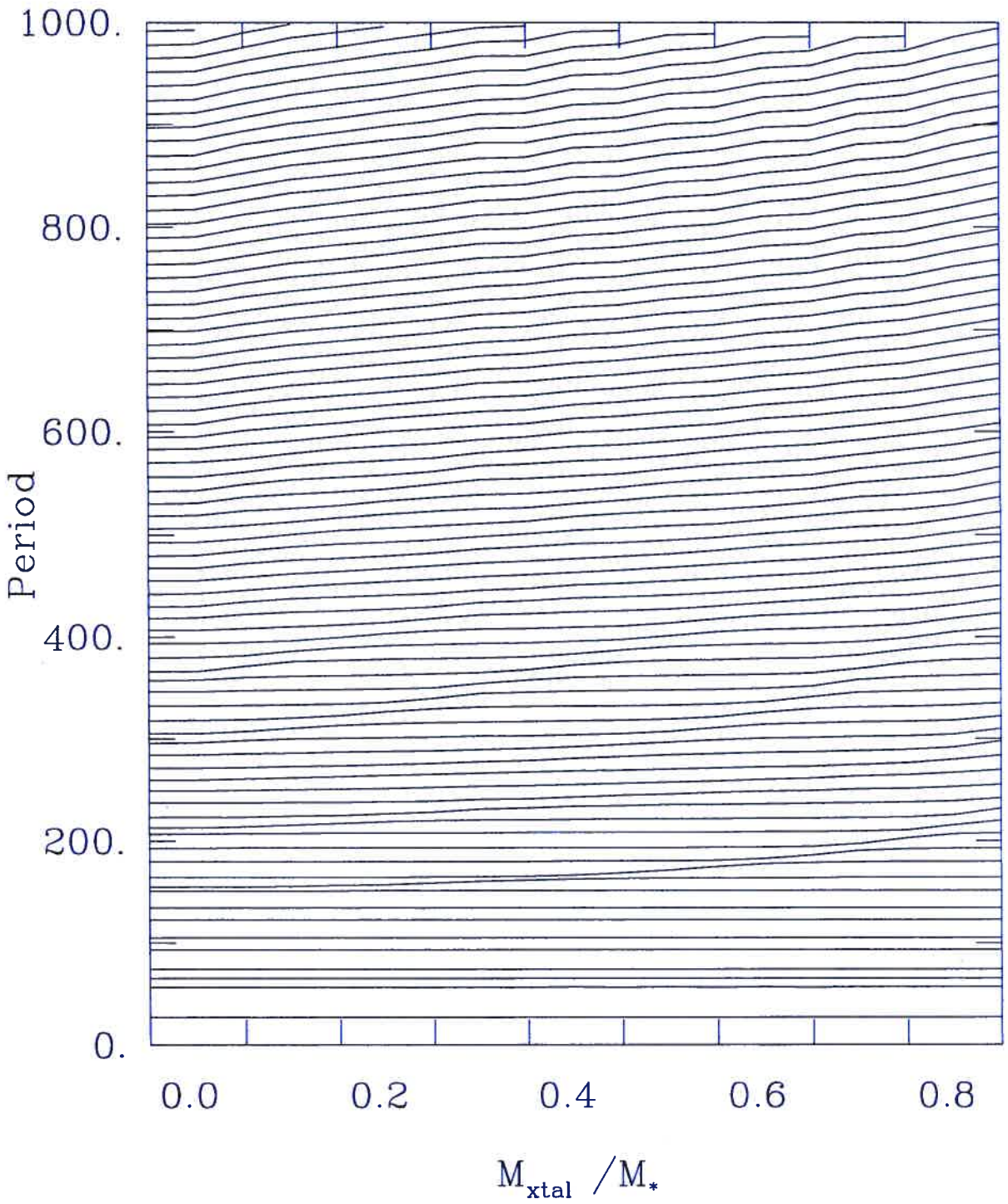

FIGURE 4.17 – Fraction of crystallization (M_{xtal}/M_*) of a model with a core composed of pure carbon vs. the period of the pulsations with wave number $l = 2$.

line represents the pulsations with wave number $l = 1$ and the dashed $l = 2$.

Physically what is occurring is the exclusion of the pulsations from the central part of the star, and since all of the pulsations modes are found within this now diminished liquid component of the system, the average period spacing between consecutive overtones and the periods of the pulsations themselves are increased. These results are consistent with the results of Montgomery & Winget (1998), who did the same calculations using different stellar models. What is more important for this research though is the actual effect to the average period spacing of varying the crystallization percentage from one extreme to the other of the used parameter space. From the above simulations it can be seen that there is a change of approximately 3 and 1.5 seconds for the $l = 1$ and $l = 2$ pulsations respectively. In the scope of the model considered here these changes are rather small but not insignificant. Thus the crystallization could possibly be an important source of uncertainty in the comparison of pulsation models to observed instabilities in BPM 37093.

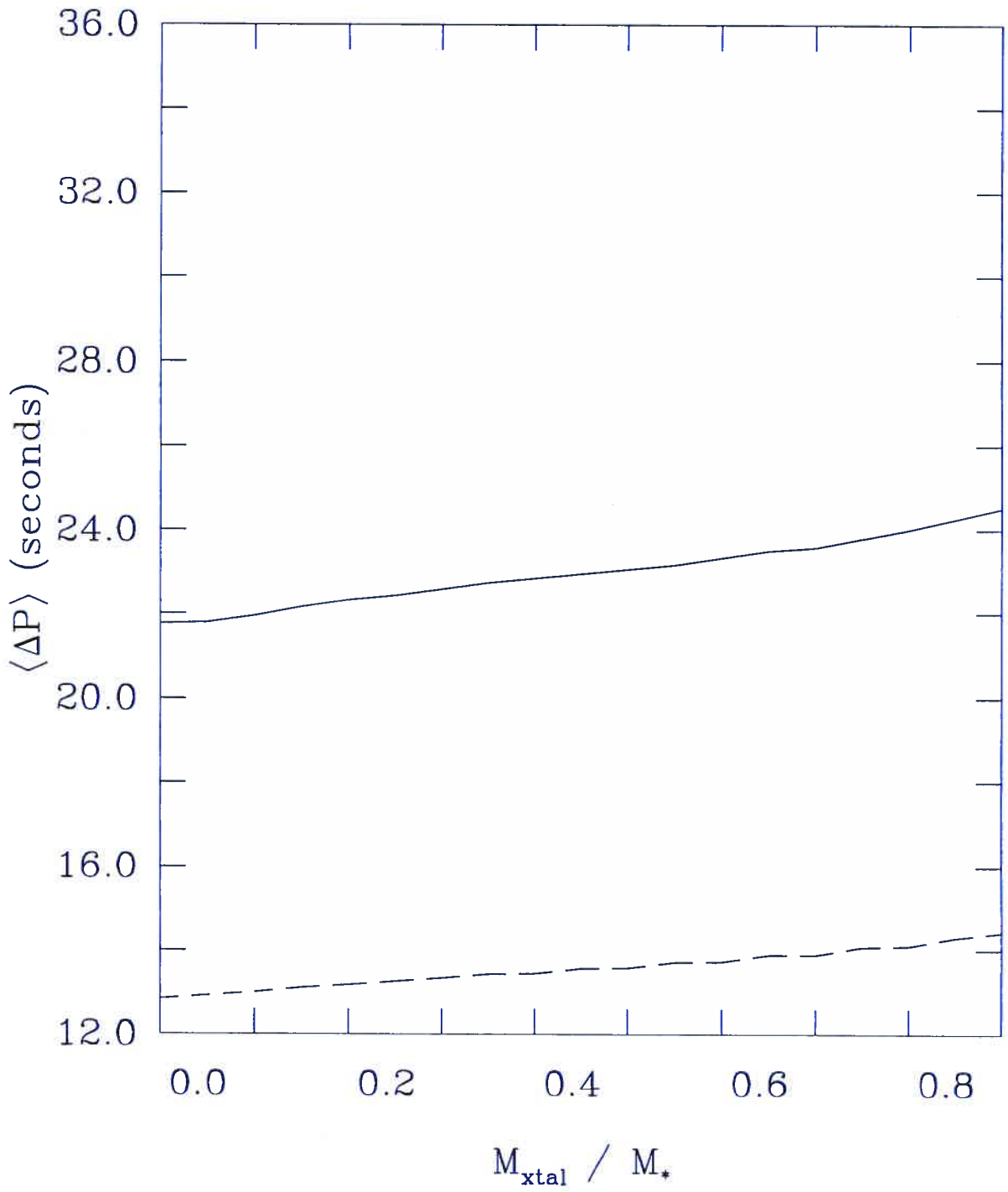

FIGURE 4.18 – Fraction of crystallization vs. the mean period spacing for a model with a core composed of 100% carbon. The solid line is for pulsations with wave number $l = 1$, while the dashed line those with wave number $l = 2$

Chapter 5

Conclusion

The variations of the stellar parameters, T_{eff}, $\log g$, $\log q(H)$, $\log q(He)$, M_{xtal}/M_*, core composition and the convective efficiency, all have an effect on the pulsations of the system. The true information from this study comes from the analysis of the relative strengths of these variables in affecting the pulsations, best compared using the average period spacing between consecutive radial overtones.

Table 5.1 is a compilation of the calculated changes in average period spacing of $l = 1$ pulsations caused by the variation of the parameters of stellar models with cores composed of an equal mixture of carbon and oxygen. From the example demonstrated in this table, and the analysis presented in chapter 4, it is obvious that some parameters can be dismissed rather quickly as competitors. The factors which appear to have the least effect on the pulsations, at least as they are varied within the range which is allocated to them for BPM 37093, are the convective efficiency, the effective temperature, and the chemical composition of the core. The first two of these cause almost no effect to the overall system, and while the third does create differences in the pulsations, its effect on the average period spacing between consecutive modes is almost nil. This last fact is best illustrated in Figure 4.6, where the average period spacings of all three of the major core compositions are compared. Therefore, the lack of knowledge of the exact values of these three parameters can be considered as very minor sources of error for the purposes of this research.

In comparing directly to the other parameters, the thickness of the helium layer seems

Stellar Parameter	Minimum value	Maximum value	$\mid < \Delta P >_{max} - < \Delta P >_{min} \mid (s)$
Convection	ML1	ML3	1.183
T_{eff}	$11,530K$	$11,930K$	0.689
$\log g$	8.76 dex	8.86 dex	1.924
$\log q(He)$	-4.0 dex	-2.0 dex	2.743
$\log q(H)$	-9.0 dex	-4.0 dex	13.226
M_{xtal}/M_*	0.0	0.9	2.548

TABLE 5.1 – Overall change in $< \Delta P >$ from the variation of each of the stellar parameters as determined by the difference between the $< \Delta P >$s of the upper, and lower limits of the allowed parameter space. These were calculated from the $l = 1$ pulsations of models with cores composed of equal amounts carbon and oxygen.

to be one of the most important when referring to its ability to influence the pulsations of the system. The problem in the consideration of this variable comes from one of the initial requirements needed for its study, that there must be a coupling between it and the thickness of the hydrogen layer. For the analysis of $\log q(He)$ there was a requirement that $\log q(H) = -6$, and as seen in Section 4.8 the difference created in the pulsations by a simple change from $\log q(H) = -4$ to -6 is very large. This situation causes problems in the direct comparison of the $< \Delta P >$ created by the variation of $\log q(He)$ to that of the other parameters. Overall when subtracting the effects caused by the lowered value of the thickness of the hydrogen layer, the effects caused by $\log q(He)$ are small but still larger then those caused by the effective temperature, the convective efficiency and the chemical composition of the core.

The mass of the star, dealt with here as the value of the surface gravity, is another parameter which can be considered as having a medium effect on the pulsations. Though the effect of varying its value does change the period spectrum the effect is not a major one in the grand scheme discussed here.

The factor whose variation has the most effect on the pulsations is definitely the thickness of the hydrogen layer. As seen in Section 4.8 the change to the average period spacing can be enormous even for a very small change in this parameter. Bar none this factor is the most important source of uncertainty in the determination of the structure of BPM 37093, since a very small error in the $\log q(H)$ could have detrimental effects to the created models, thus creating problems in comparison with observed periods.

The main purpose of this research was to determine if the crystallization of BPM 37093

has an important effect on its pulsations. As determined in Section 4.9, the effect of increasing the amount of the star which is crystallized serves to drive the periods of the pulsations as well as the average period spacing between consecutive radial overtones up. This effect is even stronger than what is determined by the variation of most of the other parameters, including the effective temperature, the core composition, the convective efficiency, the mass of the star as well as the thickness of the helium layer, though the last relation, as discussed earlier, is harder to directly determine due to the nature of the models in which the thickness of the helium layer is varied. From a determination based only on these results it could be said that the fraction of crystallization of BPM 37093 is a major determinant of the pulsations of the system. With this conclusion, it could be possible to attempt a direct comparison of the observed periods and, by reversing the method used here, determine the direct value for the ratio of the star that is crystallized. This would be a great merit for asteroseismology. Unfortunately, the real situation presented here is not quite so simple due to the enormous contribution of the thickness of the hydrogen layer to the determination of the pulsations. Figure 5.1 shows a direct comparison of the effect of the crystallization to the effect of the $\log q(H)$. The average period spacing, $< \Delta P >$ vs. the crystallization percentage is plotted for the $l = 1$ (the group found at the top of the figure) and the $l = 2$ (group at the bottom) pulsations with periods within 500-1000 seconds. Three models with different values of the thickness of the hydrogen layer are used; $\log q(H) =$, -4 (solid lines), -5 (dashed line), and -6 (dotted line).

From this figure the situation is very clear, the effect of varying the fraction of crystallization is rather small compared to the effect caused by the variation of the thickness of the hydrogen layer. In the situation for the $l = 1$ pulsations, the effect on the average period spacing of varying the star from 0 to 90% crystallized is smaller overall then changing the $\log q(H)$ from -4 to just -5. Also a variation of $\log q(H)$ from -5 to -6, is similar to a model with the $\log q(H) = -5$ where the fraction of crystallization is changed from 0.0 to 0.70. Obviously any claim made that the fraction of crystallization of BPM 37093 can be determined through numerical modellization is discredited by our lack of an exact value of the $\log q(H)$.

At this time, due to the fact that the thickness of the hydrogen layer is not known with any

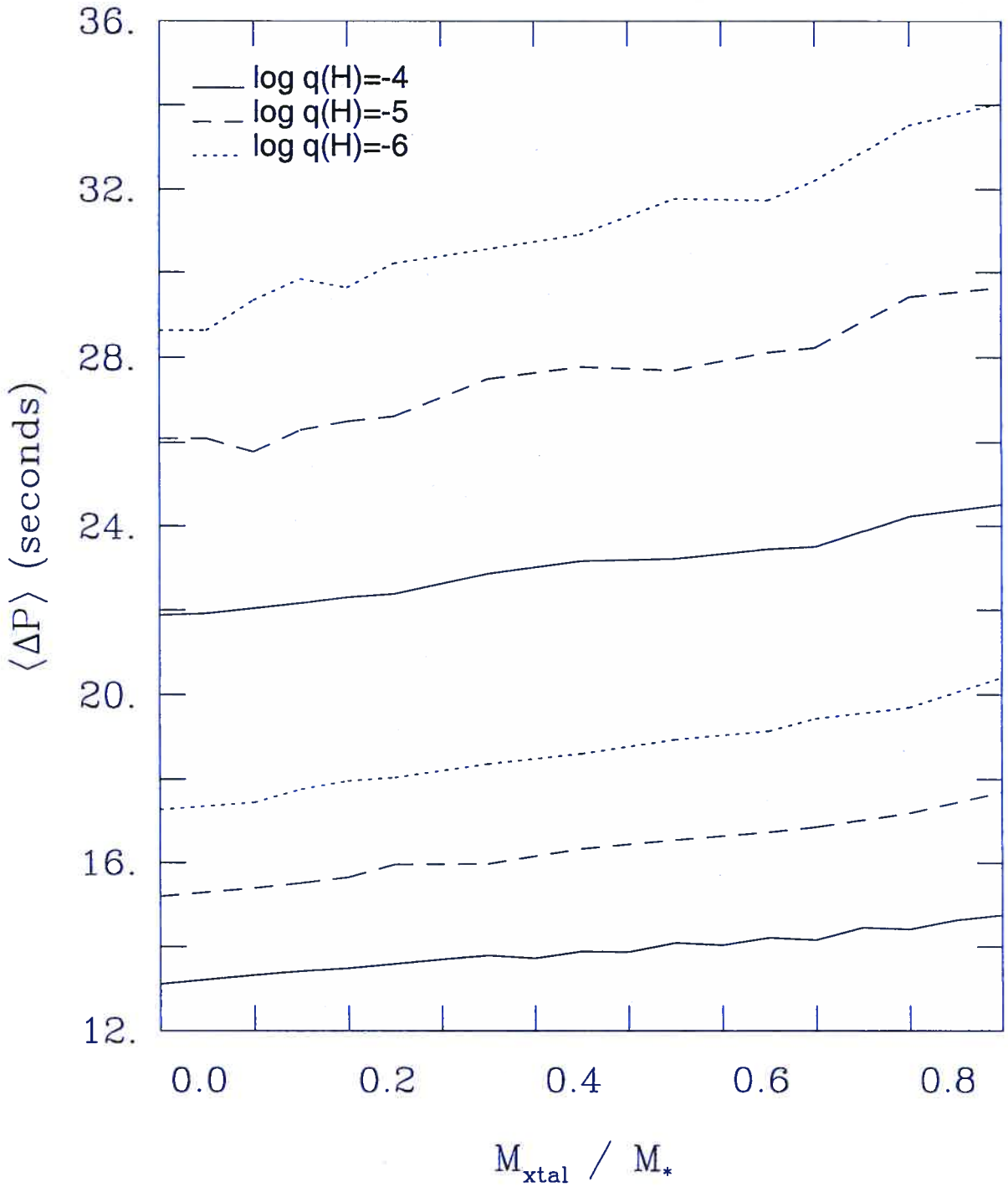

FIGURE 5.1 – Fraction of crystallization vs. the mean period spacing for a stellar model with a core composed of pure carbon. The three models represented are distingushed as follows; The solid line for a model with $\log q(H) = -4$, the dashed line for $\log q(H) = -5$, and the dotted line for $\log q(H) = -6$. The two different groups of curves are for the models with a wave number, $l = 1$ (above) and the $l = 2$ (below)

great accuracy, unfortunately this method of numerical modellization and comparison with observed periods of BPM 37093 cannot be used to determine the exact value of the fraction of crystallization. Though this does confirm that the crystallization does affect the pulsations in a significant manner compared to the other parameters of pulsation. Our inability to correctly determine another important parameter of pulsation does not allow us to capitalize on this situation so as to be able to probe the interior of BPM 37093. Indeed an unfortunate situation but one that cannot be overcome without better knowlegde of the thickness of the hydrogen layer.

Bibliography

Aizenman, M., Smeyers, P., & Weigert, A. 1977, A&A, 58, 41

Bergeron, P., Fontaine, G., Billères, M., Boudreault, S., & Green, E. M. 2004, ApJ, 600, 404

Bergeron, P. & McGraw, J. T. 1990, ApJ, 352, L45

Bergeron, P., Wesemael, F., & Fontaine, G. 1992, ApJ, 387, 288

Bergeron, P., Wesemael, F., Lamontagne, R., Fontaine, G., Saffer, R. A., & Allard, N. F. 1995, ApJ, 449, 258

Brassard, P. & Fontaine, G. 1994, in IAU Colloq. 147: The Equation of State in Astrophysics, 560–+

Brassard, P., Fontaine, G., Wesemael, F., Kawaler, S. D., & Tassoul, M. 1991, ApJ, 367, 601

Brassard, P., Fontaine, G., Wesemael, F., & Tassoul, M. 1992a, ApJS, 81, 747

Brassard, P., Pelletier, C., Fontaine, G., & Wesemael, F. 1992b, ApJS, 80, 725

Dreizler, S., Koester, D., & Heber, U. 2000, Baltic Astronomy, 9, 113

Fontaine, G., Bergeron, P., Billères, M., & Charpinet, S. 2003a, ApJ, 591, 1184

Fontaine, G., Brassard, P., & Charpinet, S. 2003b, Ap&SS, 284, 257

Fontaine, G., Lacombe, P., McGraw, J. T., Dearborn, D. S. P., & Gustafson, J. 1982, ApJ, 258, 651

Giovannini, O. 1996, Ph.D. Thesis

Hansen, C. J. & van Horn, H. M. 1979, ApJ, 233, 253

Kanaan, A., Kepler, S. O., Giovannini, O., & Diaz, M. 1992, ApJ, 390, L89

Kanaan, A., Kepler, S. O., Giovannini, O., Winget, D. E., Montgomery, M., & Nitta, A. 1998, Baltic Astronomy, 7, 183

Kanaan, A., Nitta-Kleinman, A., Winget, D. E., Kepler, S. O., Montgomery, M., & WET team. 2000, Baltic Astronomy, 9, 87

Koester, D. & Allard, N. F. 2000, Baltic Astronomy, 9, 119

Landolt, A. U. 1968, ApJ, 153, 151

McGraw, J. T. & Robinson, E. L. 1976, ApJ, 205, L155

Metcalfe, T. S., Montgomery, M. H., & Kanaan, A. 2004, ApJ, 605, L133

Montgomery, M. H. & Winget, D. E. 1998, Baltic Astronomy, 7, 197

—. 1999, ApJ, 526, 976

Nitta, A., Kanaan, A., Kepler, S. O., Koester, D., Montgomery, M. H., & Winget, D. E. 2000, Baltic Astronomy, 9, 97

Salpeter, E. E. 1961, ApJ, 134, 669

Winget, D. E., Kepler, S. O., Kanaan, A., Montgomery, M. H., & Giovannini, O. 1997, ApJ, 487, L191+

Acknowledgements

I would like to thank my research director, Gilles Fontaine, who always took the time to explain everything to me in great detail, never getting discouraged if it took longer then it should have. Though our schedules never really came together correctly, without his support, and gracious donation of time, I would have never been able to complete my research, for that I am most grateful. To Pierre Bergeron and François Wesmael, I just want to thank-you both for being such dedicated, and great teachers, your classes were defiantly the most well prepared, presented, and explained courses that I have ever taken, and it was a pleasure to take part in the experience.

For those close to my heart, I would first like to thank my two sons, Philippe and Shawn, without which I don't think I could have kept my sanity through the roughest of times, even if I probably would have slept a lot more in the mornings. Anie, I love you and adore the little family we have built together, I anxiously await our little girl to arrive in this world. Mom and Dad thank-you for everything, the amount of ways you have helped me throughout the years are too numerous to begin to mention, you most defiantly are the best parents anyone could ever ask for, and I love you both. As for Jean-François and Tamara, thank-you for all your help in everything, I'll try to be there for you as well, no matter where you will move to next.

As for all of my friends, including those who I have known for years and the other students I only met recently in my changing of schools, thank-you for all of the good times, the great conversations, and of course the tremendous amount of discussions on the most inconsequential subjects. It has been fun.